

NACA RM E54F24a



RESEARCH MEMORANDUM

EFFECT OF DESIGN OVER-ALL COMPRESSOR PRESSURE
RATIO DIVISION ON TWO-SPOOL TURBOJET-
ENGINE PERFORMANCE AND GEOMETRY

By James F. Dugan, Jr.

Lewis Flight Propulsion Laboratory
CLASSIFICATION CHANGED, Cleveland, Ohio

UNCLASSIFIED

To _____

~~CONFIDENTIAL~~

By authority of *NASA TPA 9* Date *9-1-59*
NR 11-20-59

~~CONFIDENTIAL~~
LANGLEY RESEARCH AIRCRAFT DIVISION

CLASSIFIED DOCUMENT

This material contains information affecting the National Defense of the United States within the meaning of the espionage laws, Title 18, U.S.C., Sections 793 and 794, the transmission or revelation of which in any manner to an unauthorized person is prohibited by law.

NATIONAL ADVISORY COMMITTEE FOR AERONAUTICS

WASHINGTON
September 7, 1954



NATIONAL ADVISORY COMMITTEE FOR AERONAUTICS

RESEARCH MEMORANDUMEFFECT OF DESIGN OVER-ALL COMPRESSOR PRESSURE RATIO DIVISION ON
TWO-SPOOL TURBOJET-ENGINE PERFORMANCE AND GEOMETRY

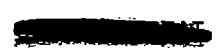
By James F. Dugan, Jr.

SUMMARY

The effect of design over-all compressor pressure ratio division on two-spool turbojet-engine performance and geometry is determined by considering three engines, each having a design over-all compressor pressure ratio, turbine-inlet temperature, and afterburner temperature of 12, 2500° R, and 3500° R, respectively. For each engine the division of over-all pressure ratio between the outer and inner compressors, respectively, is 2-6, 3-4, and 4-3. For a range of flight Mach numbers up to 2.8, full-thrust engine performance (that which results from operation at the design values of outer-spool mechanical speed and inner-turbine inlet temperature) is analytically obtained by matching compressor and turbine component performance maps. Full-thrust engine performance with and without afterburning is presented for complete expansion across the exhaust nozzle; full-thrust performance with afterburning is presented for incomplete exhaust-nozzle expansion. Cruise performance for no afterburning and complete exhaust-nozzle expansion is presented for a flight Mach number of 0.9 in the stratosphere. The component frontal areas of each engine are computed for selected component design limits.

On the basis of full-thrust and cruise performance for complete exhaust-nozzle expansion, one particular pressure ratio division has no decided advantage over any other division. However, if one-stage turbines are stipulated, minimum turbine frontal area and maximum thrust per unit frontal area for incomplete expansion are obtained by designing for an outer-compressor pressure ratio less than inner-compressor pressure ratio. Over a wide range of flight conditions, the inner turbine of each engine operated very close to its design point, the outer-turbine equivalent speed varied slightly, and specific work exceeded the design value by about 25 percent at the highest flight Mach number considered in this report, 2.8. Outer-compressor surge is more likely to occur at high flight Mach numbers; the effect of work split on this tendency is small.

UNCLASSIFIED



3357

T-SC

INTRODUCTION

In designing a two-spool turbojet engine, a decision must be made regarding the division of work between the outer and inner compressors. It is possible that, for a given over-all compressor pressure ratio, a particular division of pressure ratio between the outer and inner compressors will be more favorable than other divisions as regards full-thrust performance, cruise performance, accelerating characteristics, or engine geometry.

In reference 1, this problem is treated for a design over-all pressure ratio of 12. Horizontal compressor characteristics corresponding to a constant adiabatic efficiency of 80 percent and a temperature rise proportional to the square of the rotational speed were assumed. (Compressor pressure ratio and temperature ratio are constant for a fixed rotational speed.) Also, a reference line was used as an approximate surge line for the compressors, though (as stated in the reference) the form of the actual surge lines might easily vary with the pressure ratio of each compressor. On the assumption that the trend of the equilibrium operating lines will not be greatly changed by the adoption of more practical compressor characteristics, it was concluded that, if the engine operating lines on both high- and low-pressure compressors are to be as reasonable as possible, the work division between the two compressors should be about even; that is, pressure ratio splits of 3-4 and 4-3 appear more suitable than those of 2-6 or 6-2. This conclusion is based on the locations of the operating lines with respect to the surge lines and optimum efficiency zones of the outer and inner compressors.

In order to evaluate further the potential characteristics of two-spool engines, an analytical study of two-spool aircraft engines is now being conducted at the NACA Lewis laboratory. The over-all objective of this program is to investigate problems in the design and operation of such engines. Reference 2 presents procedures for evaluating the performance of two-spool engines once the operating characteristics of the engine components are known. The objective of the present report is to determine the effect of design work split on two-spool turbojet-engine performance and geometry. This report differs from reference 1 in that more realistic component characteristics are employed and engine performance is computed for a range of flight conditions. Three engines having sea-level take-off over-all compressor pressure ratio divisions of 2-6, 3-4, and 4-3 are considered; a pressure ratio division of 6-2 was not considered, since reference 1 indicates this work split to be the least desirable of those analyzed. Full-thrust engine performance with and without afterburning is calculated for each engine over a range of flight conditions. Full-thrust performance is defined to be that which results from engine operation at constant design outer-spool mechanical speed and constant design inner-turbine inlet temperature. Cruise performance of each engine is calculated for a flight Mach number of 0.9 in

the stratosphere. The component frontal areas of each engine are calculated for a selected set of component design limits.

SYMBOLS

The following symbols are used in this report:

A	area, sq ft
a_{cr}	critical velocity of sound, ft/sec
F	thrust, lb
g	standard gravitational acceleration, 32.2 ft/sec ²
H	stagnation enthalpy, Btu/lb
J	mechanical equivalent of heat, 778.2 ft-lb/Btu
M	Mach number
N	rotational speed, rpm
P	total pressure, lb/sq ft
r	radius, ft
sfc	specific fuel consumption, (lb fuel)/(hr)(lb thrust)
T	total temperature, °R
U	wheel speed, ft/sec
V	velocity, ft/sec
W	weight flow, lb/sec
δ	ratio of total pressure to NACA standard sea-level pressure, P/2116
η	adiabatic efficiency
θ	ratio of total temperature to NACA standard sea-level temperature, T/518.4
σ	ratio of total density to NACA standard sea-level density
ω	angular velocity, radians/sec

Subscripts:

- b backbone
- d design
- f fuel
- h hub
- i inner-spool
- n net
- o outer-spool
- s surge
- x axial
- 0 ambient conditions
- 1 outer-compressor inlet
- 2 outer-compressor exit, inner-compressor inlet
- 3 inner-compressor exit, combustor inlet
- 4 combustor exit, inner-turbine inlet
- 5 inner-turbine exit, outer-turbine inlet
- 6 outer-turbine exit, afterburner inlet
- 7 exhaust-nozzle exit

Numerical subscripts are shown on fig. 1.

METHOD OF ANALYSIS

Figure 1 presents a cross section of a two-spool turbojet engine showing the location of the numerical stations. Three two-spool turbojet engines are discussed in this report. They are designated engines 26, 34, and 43, the first and second numerals of each number specifying the static sea-level compressor total-pressure ratios of the outer and inner compressors, respectively. The design conditions (those for static sea-level engine operation) common to all three engines are as follows:

Over-all compressor pressure ratio	12
Outer-compressor equivalent weight flow, lb/sec	150
Outer- and inner-compressor polytropic efficiency, percent	90
Inner-turbine inlet temperature, °R	2500
Inner- and outer-turbine adiabatic efficiency, percent	87
Afterburner temperature, °R	3500

Component Performance

In order to investigate the effect of design over-all compressor pressure ratio division on two-spool turbojet-engine performance, it is necessary to obtain representative compressor and turbine component performance maps. The component maps used herein are believed to be realistic approximations of the actual performance maps of components having the same design values.

Compressor. - The method of obtaining the compressor maps for the two-spool engines is based on the material presented in reference 3, which describes a procedure for estimating the performance of a compressor having blading similar to that of an existing compressor but different design conditions.

Each of the compressor maps presented herein was constructed as follows: The compressor backbone was computed; the compressor surge line was calculated; and the constant-speed lines were constructed. The backbone of a compressor map is defined as the line of maximum efficiencies. Its shape is believed to be dependent primarily on the design value of compressor pressure ratio. Compressor design values, as used herein, are defined as those corresponding to peak polytropic efficiency. The backbones of six compressors having design pressure ratios from 2.08 to 9.20 were determined. From these data was constructed figure 2, which shows the effect of design pressure ratio on backbone pressure ratio, weight flow, and efficiency for constant values of equivalent speed. The backbone of a desired compressor map was computed by multiplying the values read from figure 2 by the appropriate design values.

The shape of the compressor surge line was assumed to depend only on the design value of compressor pressure ratio. Surge data on the six compressors referred to in the previous paragraph yielded figure 3, a plot of surge pressure ratio (percent design) against design pressure ratio for constant values of surge weight flow (percent design). The surge line of a desired compressor map was calculated by multiplying the values read from figure 3 by the appropriate design values. Surge lines estimated in this manner are continuous; whereas, the surge lines of actual compressors are discontinuous (ref. 4). It is believed that this discrepancy does not seriously affect the analysis, because, for design pressure ratios from 2 to 6, the surge-line discontinuity probably occurs at an equivalent speed less than 70-percent design, the minimum compressor speed considered in this report.

The constant-speed characteristics of a compressor may be obtained from its performance map by computing the temperature rise, adiabatic efficiency, and flow parameter of each point; these values are divided by the appropriate backbone values and yield constant-speed characteristics that are independent of speed. Such constant-speed characteristics are believed to depend primarily on the aerodynamic limits employed in designing the compressor. The constant-speed lines of a desired compressor map were constructed by using figure 4, a plot of the constant-speed characteristics of a compressor designed for aerodynamic limits similar to those listed in the Engine Geometry section. For selected values of the flow parameter, values of relative efficiency and relative temperature rise were read. For each speed, values of pressure ratio, efficiency, and equivalent weight flow were calculated from values read from figure 4 and the backbone values previously calculated.

Turbine. - Each of the turbine maps used in this investigation was derived from the performance map of the one-stage turbine discussed in reference 5. A desired turbine map was constructed by multiplying the reference turbine parameters by the appropriate ratio of the design value of the desired turbine to the design value of the reference turbine. In fairing in the turbine efficiency contours in the upper part of the turbine map, consideration was given to the fact that, for a specific value of design exit axial-velocity ratio, as design specific work decreases, the ratio of specific work at limiting loading to design specific work increases. In relating the specific work at limiting loading to design specific work, it was assumed that the turbine-exit axial-velocity ratio was 0.5 at design and 0.7 at the limiting-loading condition. It was also assumed that the turbine efficiencies of the derived turbine maps at design and at limiting loading were the same as those of the reference turbine map. For each derived turbine map, an estimated line of limiting loading was faired through the limiting-loading point at design equivalent speed.

Engine Performance for Complete Exhaust-Nozzle Expansion

For the three two-spool turbojet engines considered herein, the compressor and turbine component performance maps were matched together, by the method described in reference 2, to determine over-all engine performance. In matching the components of each engine to obtain pumping characteristics, it was assumed that the amount of air required to cool the turbines is equal to the amount of fuel added in the primary burner and that this cooling air is bled from the inner-compressor discharge; constant values of pressure ratio across the primary burner and afterburner were assumed. For full-thrust operation, the outer-spool mechanical speed and the inner-turbine inlet temperature were maintained constant at their design values. Full-thrust performance with and without afterburning was calculated for flight Mach numbers from 0 to 0.9 at sea level and 0.9 to 2.8 in the stratosphere.

Cruise performance for each engine was computed for a flight Mach number of 0.9 in the stratosphere. Constant outer-spool speed curves of specific fuel consumption against an equivalent net thrust parameter were determined by varying the turbine-inlet temperature at each equivalent speed. The envelope of these constant-speed curves specifies the minimum specific fuel consumption attainable at various thrust levels for the specified cruise Mach number. The altitude and thrust requirement for cruise may be selected once the variation of airplane lift-drag ratio with altitude is known.

Engine Geometry

The geometry of each engine was computed for the following component design values and a specified variation of axial velocity with compressor pressure ratio:

Air flow per unit frontal area at station 1, lb/(sec)(sq ft) . . .	35
Outer-compressor tip speed, ft/sec	1100
Outer-compressor entrance axial Mach number	0.6
Inner-compressor first-rotor tip relative Mach number	1.18
Inner-compressor exit axial velocity, ft/sec	500
Inner- and outer-compressor exit tangential velocity, ft/sec . . .	0
Inner-turbine exit axial-velocity ratio, $V_{x,5}/a_{cr,5}$	0.5
Number of inner-turbine stages	1
Inner-turbine loading parameter, $Jg(H_4-H_5)/U_{h,5}^2$	2.1
Outer-turbine exit axial-velocity ratio, $V_{x,6}/a_{cr,6}$	0.5
Number of outer-turbine stages	1
Outer-turbine loading parameter, $Jg(H_5-H_6)/U_{h,6}^2$	2.1
Primary-combustor maximum velocity, ft/sec	125
Primary-combustor hub-tip radius ratio	0.4
Afterburner maximum velocity, ft/sec	550

Compressor frontal area was calculated from the values of air flow and air flow per unit frontal area; constant rotor tip radius was assumed throughout the outer and inner compressors. Values of outer-compressor tip speed and entrance axial Mach number yielded values of rotor tip relative Mach number and hub-tip radius ratio.

Inner-spool tip speed was calculated from the values of axial velocity and rotor tip relative Mach number at the entrance of the inner spool.

From cycle calculations and the selected value of turbine-exit axial-velocity ratio, the exit annulus area of each turbine was computed. Calculations involving reference 6 indicate that the stage-loading parameter of a conservatively designed one-stage turbine may be as high as 2.1. From values of turbine specific work, stage-loading parameter, and

angular velocity, the hub radius of each turbine was calculated. This value, together with the value of annulus area, determined the frontal area of each turbine; constant rotor tip radius was assumed for each turbine. Rotor blade hub centrifugal stresses were calculated for assumed values of blade taper factor and density of material of 0.7 and 490 pounds per cubic foot, respectively.

The primary-combustor frontal area compatible with the specified values of hub-tip radius ratio and velocity was calculated for flight Mach numbers of 0 and 0.9 at sea level and 0.9 and 2.8 in the stratosphere. For the same four flight conditions, afterburner frontal area was determined for the specified afterburner velocity; exhaust-nozzle area was calculated for complete expansion with afterburning; and free-stream area was determined for values of inlet pressure recovery read from figure 5, a plot of pressure recovery against Mach number for a two-wedge variable inlet.

Engine Performance for Incomplete Exhaust-Nozzle Expansion

The large exhaust nozzles required for complete expansion at a flight Mach number of 2.8 are believed to be impractical. Therefore, calculations were made in which the maximum exhaust-nozzle area was limited to the maximum frontal area of the other components. Engine thrust and specific fuel consumption were computed for engine operation with 2500° R primary-combustor temperature and 3500° R afterburner temperature.

RESULTS AND DISCUSSION

Component Performance

The component performance maps obtained by the methods discussed in the previous section are shown in figures 6 to 9. Plotted on each compressor and turbine component map is the full-thrust line for engine operation at constant values of outer-spool mechanical speed (the design value) and inner-turbine inlet temperature (2500° R) over the full range of flight conditions. Flight conditions of sea-level take-off, Mach 0.9 in the stratosphere, and Mach 2.8 in the stratosphere (points A, B, and C, respectively) are noted on each full-thrust operating line. Sea-level flight at Mach 0.9 lies on the operating line between points A and C. The operating line on the component map is not affected by the use of afterburning. Once the components of the engine are matched, each component operating point at any flight condition is uniquely determined by the mode of operation. For the present case, the flight condition and operating mode (constant N_o and T_4) give values of outer-spool equivalent speed $N_o/\sqrt{\theta_1}$ and turbine-to-compressor temperature ratio T_4/T_1 that determine the operating point of each component.

Compressor. - The outer-compressor performance maps of engines 26, 34, and 43 are shown in figures 6(a), (b), and (c), respectively. For each engine, the outer-compressor efficiency is 85 percent or higher over most of the flight range. For operation in the stratosphere, as flight Mach number increases the outer-compressor operating point moves closer to the surge region, so that at high flight Mach numbers there is only a small margin between the surge line and the equilibrium operating line. Therefore, the probability of surging the outer compressor is greater when the two-spool engine is operating at high flight Mach numbers; the effect of work split does not appear to be significant in this respect.

The inner-compressor performance maps of engines 26, 34, and 43 are plotted in figures 7(a), (b), and (c), respectively. As was the case for the outer compressors, the inner-compressor efficiency of each engine is 85 percent or higher over most of the flight range. For operation in the stratosphere, as flight Mach number increases the inner-compressor operating point moves away from the surge region.

Turbine. - The turbine maps of the two-spool engines are shown in figures 8 and 9 as plots of equivalent specific work $\Delta H/\theta$ against an equivalent flow parameter WN/δ for constant values of equivalent speed and efficiency. An estimated limiting-loading line is shown on each map.

The inner-turbine maps of engines 26, 34, and 43 are shown in figures 8(a), (b), and (c), respectively. On each of these maps, it is evident that inner-turbine operation over the complete range of flight conditions is confined to a small region of the performance map. Equivalent speed, specific work, and efficiency vary only a small percentage of their design values.

The outer-turbine performance maps of engines 26, 34, and 43 are shown in figures 9(a), (b), and (c), respectively. The range of equivalent speed covered by the engine operating line is small, because outer-spool mechanical speed and inner-turbine inlet temperature are constant and inner-turbine temperature ratio varies only slightly, as evidenced by the small variation in inner-turbine specific work. The outer-turbine specific-work range covered by the engine operating line is considerably larger than that of the inner turbine. As flight Mach number increases, outer-turbine specific work increases. At a flight Mach number of 2.8 in the stratosphere (point C), design specific work is exceeded by about 25 percent. This indicates that the outer turbine should be designed for a conservative exit axial-velocity ratio to ensure that limiting loading will not be encountered at high flight Mach numbers. The margin between operating point C and the estimated limiting-loading line is small for engine 43 and considerably larger for engines 34 and 26. This indicates that specifying a design outer-turbine exit axial-velocity ratio of 0.5 is adequate for engine 43 and more than adequate for engines 34 and 26.

Engine Performance for Complete Exhaust-Nozzle Expansion

Full-thrust operation. - The full-thrust performance with afterburning of engines 26, 34, and 43 over the complete range of flight conditions is shown in figure 10. For Mach numbers from 0 to 0.9, operation is at sea level; operation is in the stratosphere for flight Mach numbers from 0.9 to 2.8. Equivalent net thrust per unit design air flow is plotted against flight Mach number in figure 10(a). For operation at sea level, all three engines give the same thrust values. The variation in thrust among the three engines for operation in the stratosphere is between 2 and 6 percent. Specific fuel consumption is plotted against flight Mach number in figure 10(b). During sea-level operation, the variation of specific fuel consumption among the engines is of the order of 1 percent. The variation is about the same for operation in the stratosphere up to a flight Mach number of 2.0. The maximum variation occurs at a Mach number of 2.8, where engines 26 and 34 have about 4.5-percent-lower specific fuel consumption than engine 43.

The full-thrust performance without afterburning is shown in figure 11. Equivalent net thrust per unit design air flow is plotted against flight Mach number in figure 11(a). For sea-level operation, the maximum thrust variation among the engines is about 4 percent, engines 26 and 34 exhibiting slightly higher thrust values. For operation in the stratosphere, the thrust of engine 26 is about 2.5 percent higher than that of engine 43 for flight Mach numbers from 0.9 to 1.8. The maximum thrust difference occurs at a Mach number of 2.8, where engine 26 has about 9-percent-greater thrust than engine 43. At this flight condition, the weight flows and over-all compressor pressure ratios of the two engines are the same, while the jet velocity of engine 26 exceeds that of engine 43 by about 2 percent because of slight differences in component efficiencies. At the higher flight Mach numbers, as the jet velocity approaches the flight velocity, net thrust becomes more sensitive to changes in jet velocity; at Mach 2.8 in the stratosphere, the 2-percent difference in jet velocity between engines 26 and 43 results in the 9-percent difference in net thrust.

Specific fuel consumption is plotted against flight Mach number in figure 11(b). The minimum value of specific fuel consumption at static sea-level conditions is 1.0. The minimum specific fuel consumption attainable for a turbine temperature of 2500° R is, of course, smaller than 1.0, but a compressor pressure ratio much greater than 12 is required to obtain this value. The maximum variation of specific fuel consumption during sea-level operation is less than 3 percent, with engine 43 exhibiting the smallest specific fuel consumption at each flight Mach number. For operation in the stratosphere, minimum specific fuel consumption is attained by engine 43 for flight Mach numbers of 0.9 to 1.9 and by engine 26 for Mach numbers above 1.9. Over most of the Mach number range in the stratosphere, the variation of specific fuel consumption is less

than 3 percent. The variation increases at the higher flight Mach numbers; at a Mach number of 2.8, the specific fuel consumption of engine 43 is about 6.5 percent higher than that of engine 26. At the higher flight Mach numbers, specific fuel consumption is also sensitive to changes in jet velocity.

Over much of the flight range, the differences in full-thrust performance with complete exhaust-nozzle expansion among the three engines are 4 percent or less. Larger differences (up to 9 percent) exist at the highest flight Mach number considered. These differences, however, result from slight differences in component efficiencies and are within the variations that may be expected from varying the match point of a given set of components. The effect of design over-all compressor pressure ratio division on full-thrust performance with or without afterburning and with complete exhaust-nozzle expansion does not appear to be appreciable.

Cruise operation. - Cruise performance at a flight Mach number of 0.9 in the stratosphere is shown in figure 12 as a plot of minimum specific fuel consumption against equivalent net thrust per unit design air flow for engines 26, 34, and 43. Each of the curves shown in figure 12 is the envelope of constant outer-spool speed curves (specific fuel consumption against equivalent net thrust per unit design air flow) obtained by varying the turbine-inlet temperature at each equivalent speed. The lowest value of minimum specific fuel consumption, 1.125, is attained by engine 43; the lowest values for engines 34 and 26 are 1.133 and 1.150, respectively. Each engine attains its lowest specific fuel consumption at a different level of thrust. The thrust level and altitude for the cruise condition are selected by considering the variation of airplane lift-drag ratio with altitude as well as the variation of minimum specific fuel consumption with equivalent net thrust. The effect of over-all compressor pressure ratio division on two-spool turbojet-engine cruise performance appears to be small.

Engine Geometry

The component design values calculated from the specific component design limits are as follows:

3367

CS-2 back

Component value	Engine		
	26	34	43
Outer-compressor frontal area, sq ft	4.29	4.29	4.29
Outer-compressor first-rotor tip relative Mach number	1.18	1.18	1.18
Outer-compressor first-rotor hub-tip radius ratio	0.39	0.39	0.39
Inner-compressor frontal area, sq ft	4.29	4.29	4.29
Inner-compressor tip speed, ft/sec	1281	1415	1510
Inner-compressor first-rotor hub-tip radius ratio	0.70	0.78	0.82
Inner-turbine frontal area, sq ft	5.52	4.05	3.19
Inner-turbine hub-tip radius ratio	0.82	0.78	0.75
Inner-turbine centrifugal stress at rotor hub, psi	25,800	27,000	27,300
Outer-turbine frontal area, sq ft	3.58	4.47	5.18
Outer-turbine hub-tip radius ratio	0.60	0.70	0.75
Outer-turbine centrifugal stress at rotor hub, psi	23,800	23,800	23,800
Primary-combustor frontal area, sq ft	4.17	4.22	4.28
Afterburner frontal area, sq ft	4.04	4.19	4.26
Exhaust-nozzle area for complete expansion at $M_0 = 2.8$, sq ft	9.94	10.00	10.20
Free-stream area at $M_0 = 2.8$, sq ft	4.29	4.26	4.24

One-stage-turbine frontal areas. - One-stage inner-turbine frontal area exceeds compressor frontal area only for engine 26. Inner-turbine frontal area, however, can be reduced quite conveniently without going to two stages. Turbine hub radius is calculated from the following equation:

$$r_h = \frac{1}{\omega} \left(\frac{Jg\Delta H}{2.1} \right)^{1/2} \quad (1)$$

From equation (1), it is apparent that turbine hub radius (and hence turbine frontal area) decreases as angular velocity and stage-loading parameter increase. Inner-spool angular velocity may be increased without exceeding the specified inner-compressor relative entrance tip Mach number by specifying exit whirl at the discharge of the outer compressor in the direction of inner-spool rotation. The turbine stage-loading parameter may be increased by incorporating exit whirl at the discharge of the inner turbine; turbine-exit whirl should be opposite the direction of inner-spool rotation. Turbine frontal area may also be decreased by increasing the design value of exit axial-velocity ratio, which decreases the turbine annulus area. Of the three schemes for decreasing inner-turbine frontal area, incorporating exit whirl at the inner-turbine discharge appears to be the most attractive. Increasing the inner-spool angular velocity increases the stress level throughout the inner spool, while increasing the design turbine-exit axial-velocity ratio usually

decreases turbine efficiency. For the present case, increasing the inner-turbine stage-loading parameter $Jg\Delta H/U_h^2$ from 2.1 to 3.15 by incorporating exit whirl reduced the frontal area of the inner turbine from 5.52 to 4.29 square feet, the required compressor frontal area.

The one-stage outer-turbine frontal areas of engines 34 and 43 exceed compressor frontal area by about 4 and 21 percent, respectively. The same schemes may be used to reduce outer-turbine frontal area as were discussed for reducing inner-turbine frontal area. Each scheme, however, is less attractive when used to reduce outer-turbine frontal area. Incorporating exit whirl at the outer-turbine discharge is undesirable, in that energy associated with this exit whirl is lost. Such is not the case when exit whirl is incorporated at the inner-turbine discharge. Increasing outer-spool angular speed, besides increasing the outer-spool stress level, may require the use of outer-compressor inlet guide vanes. Increasing the outer-turbine exit axial-velocity ratio lowers the specific-work values at which limiting loading is encountered; this is more harmful to the outer than to the inner turbine because of the larger range of operation required by the former.

Component frontal areas dependent on flight conditions. - The free-stream, combustor, afterburner, and exhaust-nozzle areas required to satisfy the specified design limits were found to be largest for flight at M_0 of 2.8 in the stratosphere. For each engine, free-stream area is slightly less than compressor frontal area. The primary-combustor frontal areas (required to give a combustor velocity of 125 ft/sec) are approximately 97, 98, and 99 percent of the compressor frontal area for engines 26, 34, and 43, respectively. The afterburner frontal areas (required to give an afterburner velocity of 550 ft/sec) of engines 26, 34, and 43 are approximately 94, 98, and 99 percent of compressor frontal area, respectively. For each engine, exhaust-nozzle area (for complete expansion with afterburning at a flight Mach number of 2.8 in the stratosphere) is about 2.3 times the compressor frontal area.

Engine Performance for Incomplete Exhaust-Nozzle Expansion

The following is applicable only when each turbine comprises one stage. Design area of an engine is defined to be the maximum frontal area of the components upstream of the exhaust nozzle; the exhaust-nozzle area is restricted to values no greater than the design area. For engine 26, exit whirl is assumed to be incorporated at the inner-turbine discharge so that the inner-turbine frontal area is 4.29 square feet. The frontal areas of all other components are those listed in the table of the Engine Geometry section. The design areas of engines 26, 34, and 43 are 4.29, 4.47, and 5.18 square feet, respectively. Full-thrust performance with afterburning for the three engines (assuming

the exhaust-nozzle area to be no larger than the largest engine component frontal area) is presented in figure 13 as plots of equivalent net thrust per unit design area (fig. 13(a)) and specific fuel consumption (fig. 13(b)) against flight Mach number. For sea-level operation, figure 13(a) shows that engine 26 has thrust-parameter values about 3 percent greater than engine 34 and about 22 percent greater than engine 43. For stratosphere operation, the thrust-parameter value for engine 26 at M_0 of 0.9 is about 5 percent greater than that for engine 34 and about 24 percent greater than that for engine 43; at M_0 of 2.8, the thrust-parameter value for engine 26 is 3 percent greater than that for engine 34 and about 18 percent greater than that for engine 43. Figure 13(b) shows that the values of specific fuel consumption are about the same for the three engines. Minimum turbine frontal area and maximum thrust per unit frontal area are obtained by designing for an outer-compressor pressure ratio less than inner-compressor pressure ratio. The advantage in thrust parameter and turbine frontal area exhibited by engine 26 would disappear if two-stage outer turbines were specified for engines 34 and 43, rather than one-stage outer turbines.

Below flight Mach numbers of around 1.2, the exhaust-nozzle area required for complete expansion is less than the design area. For engine 26, at M_0 of 2.8, thrust for incomplete expansion is only 18.5 percent less than that for complete expansion; whereas the exhaust-nozzle area for incomplete expansion is about 57 percent less than that for complete expansion.

SUMMARY OF RESULTS

From an analytical investigation to determine the effect of overall compressor pressure ratio division on two-spool turbojet-engine performance and geometry, the following results were obtained:

1. On the basis of full-thrust and cruise performance for complete exhaust-nozzle expansion, one particular pressure ratio division has no decided advantage over any other.
2. Minimum turbine frontal area and maximum thrust per unit frontal area for incomplete exhaust-nozzle expansion are obtained by designing for an outer-compressor pressure ratio less than inner-compressor pressure ratio; this is true only if one-stage turbines are stipulated.
3. The effect of pressure ratio division on the frontal area of the inlet, the combustor, the afterburner, and the exhaust nozzle for complete expansion is small.
4. The likelihood of surging the outer compressor is greater at high flight Mach numbers; the effect of pressure ratio division on this tendency is small.

5. Over the complete range of flight conditions, the inner turbine of each engine operates very close to its design point.

6. The outer-turbine equivalent-speed range is small, while specific work exceeds design by about 25 percent at a flight Mach number of 2.8 in the stratosphere for the pressure ratio divisions considered.

Lewis Flight Propulsion Laboratory
National Advisory Committee for Aeronautics
Cleveland, Ohio, June 29, 1954

REFERENCES

1. Mallinson, D. H., and Lewis, W. G. E.: Performance Calculations for a Double-Compound Turbojet Engine of 12:1 Design Compressor Pressure Ratio. R. & M. No. 2645, British A.R.C., 1952. (Supersedes Rep. R.19, British N.G.T.E.)
2. Dugan, James F., Jr.: Two-Spool Matching Procedures and Equilibrium Characteristics of a Two-Spool Turbojet Engine. NACA RM E54F09, 1954.
3. Howell, A. R., and Bonham, R. P.: Over-All and Stage Characteristics of Axial Flow Compressors. Proc. Inst. Mech. Eng., vol. 163, 1950, pp. 235-248.
4. Benser, William A.: Analysis of Part-Speed Operation for High-Pressure-Ratio Multistage Axial-Flow Compressors. NACA RM E53I15, 1953.
5. Heaton, Thomas R., Forrette, Robert E., and Holeski, Donald E.: Investigation of a High-Temperature Single-Stage Turbine Suitable for Air Cooling and Turbine Stator Adjustment. I - Design of Vortex Turbine and Performance with Stator at Design Setting. NACA RM E54C15, 1954.
6. Cavicchi, Richard H., and English, Robert E.: A Rapid Method for Use in Design of Turbines within Specified Aerodynamic Limits. NACA TN 2905, 1953.

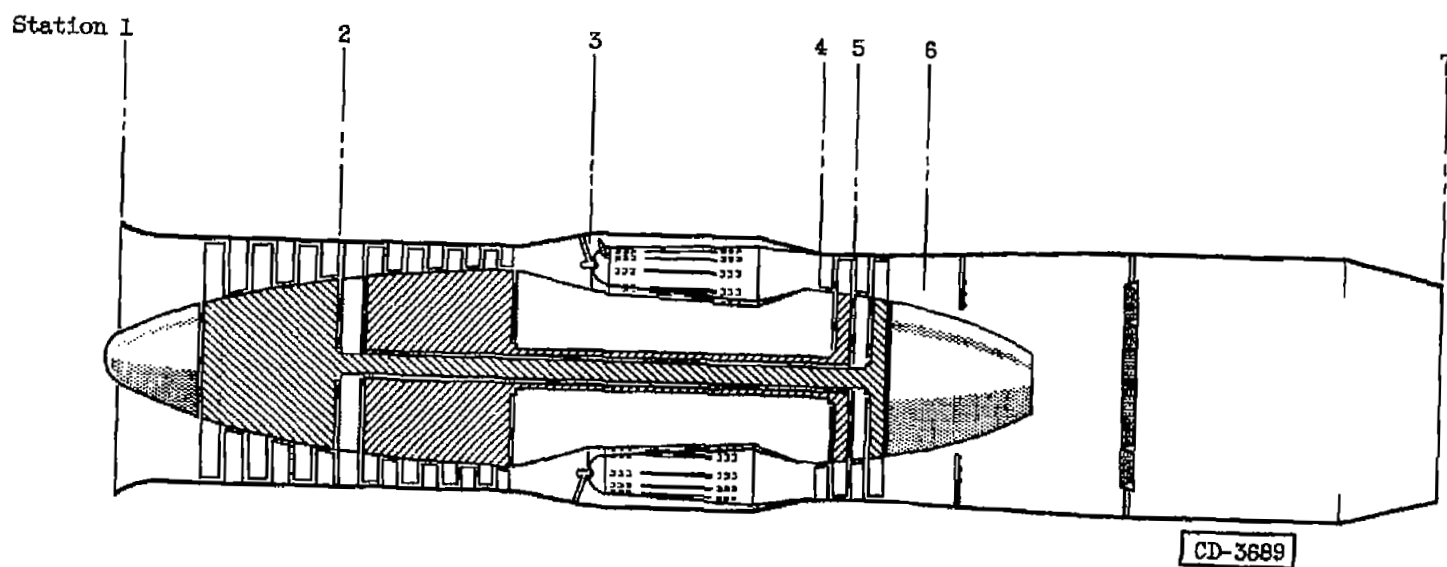
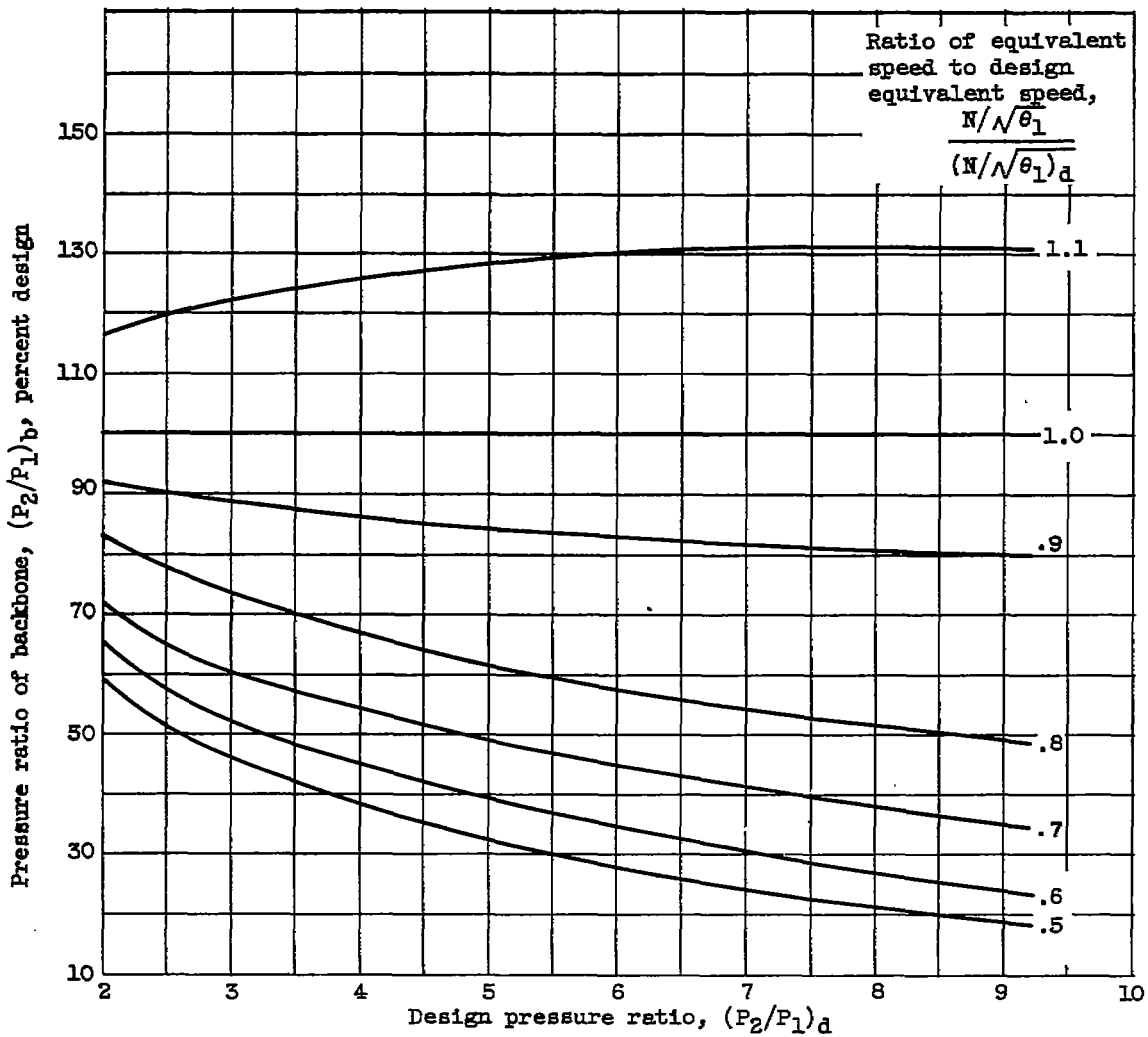


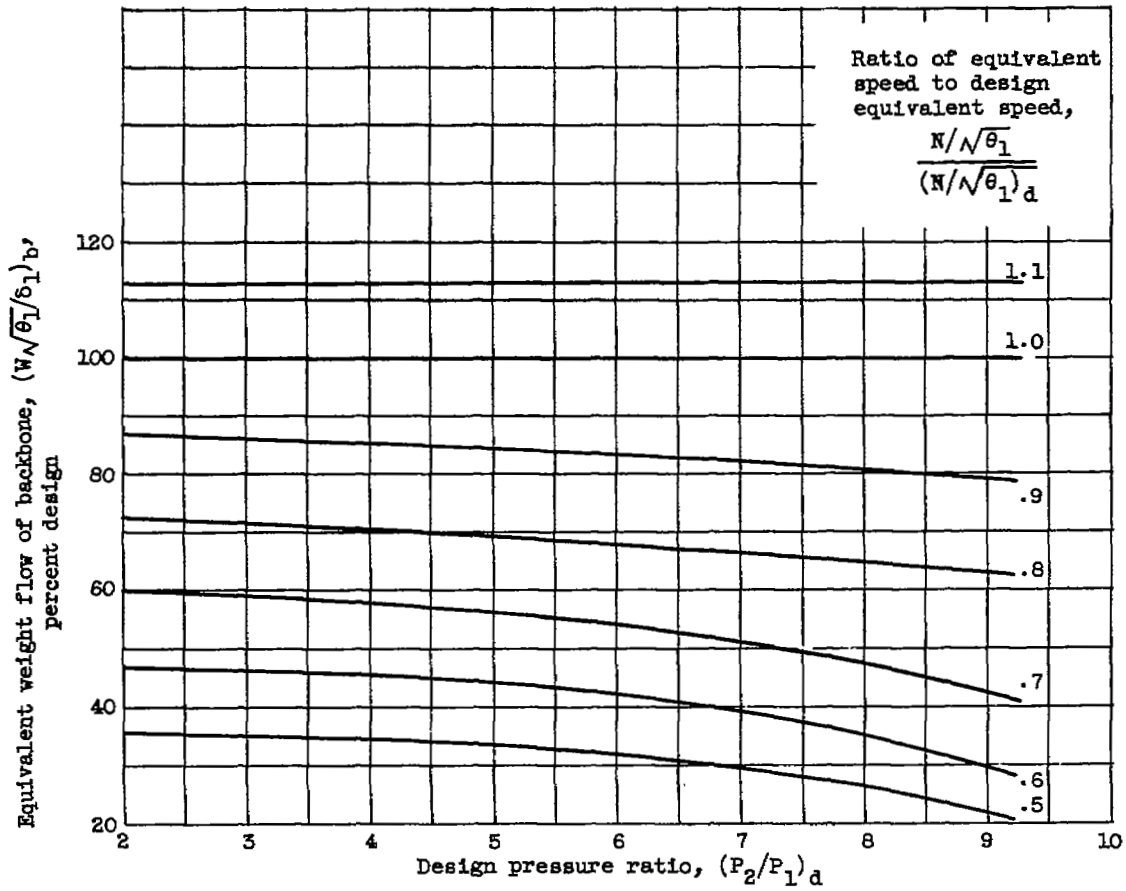
Figure 1. - Cross section of two-spool turbojet engine showing location of numerical stations.

3367
CS-3



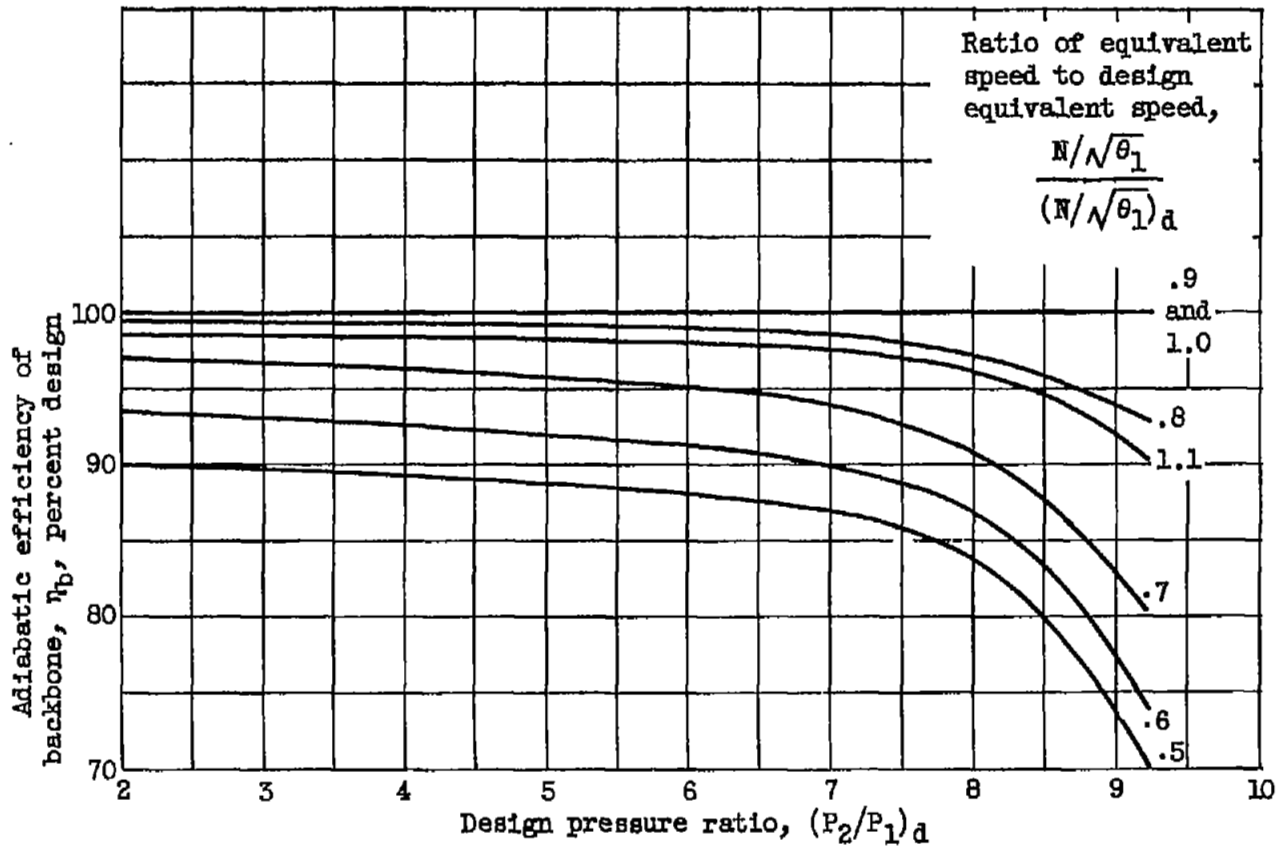
(a) Pressure ratio.

Figure 2. - Effect of design pressure ratio on backbone characteristics.



(b) Equivalent weight flow.

Figure 2. - Continued. Effect of design pressure ratio on backbone characteristics.



(c) Adiabatic efficiency.

33

Figure 2. - Concluded. Effect of design pressure ratio on backbone characteristics.

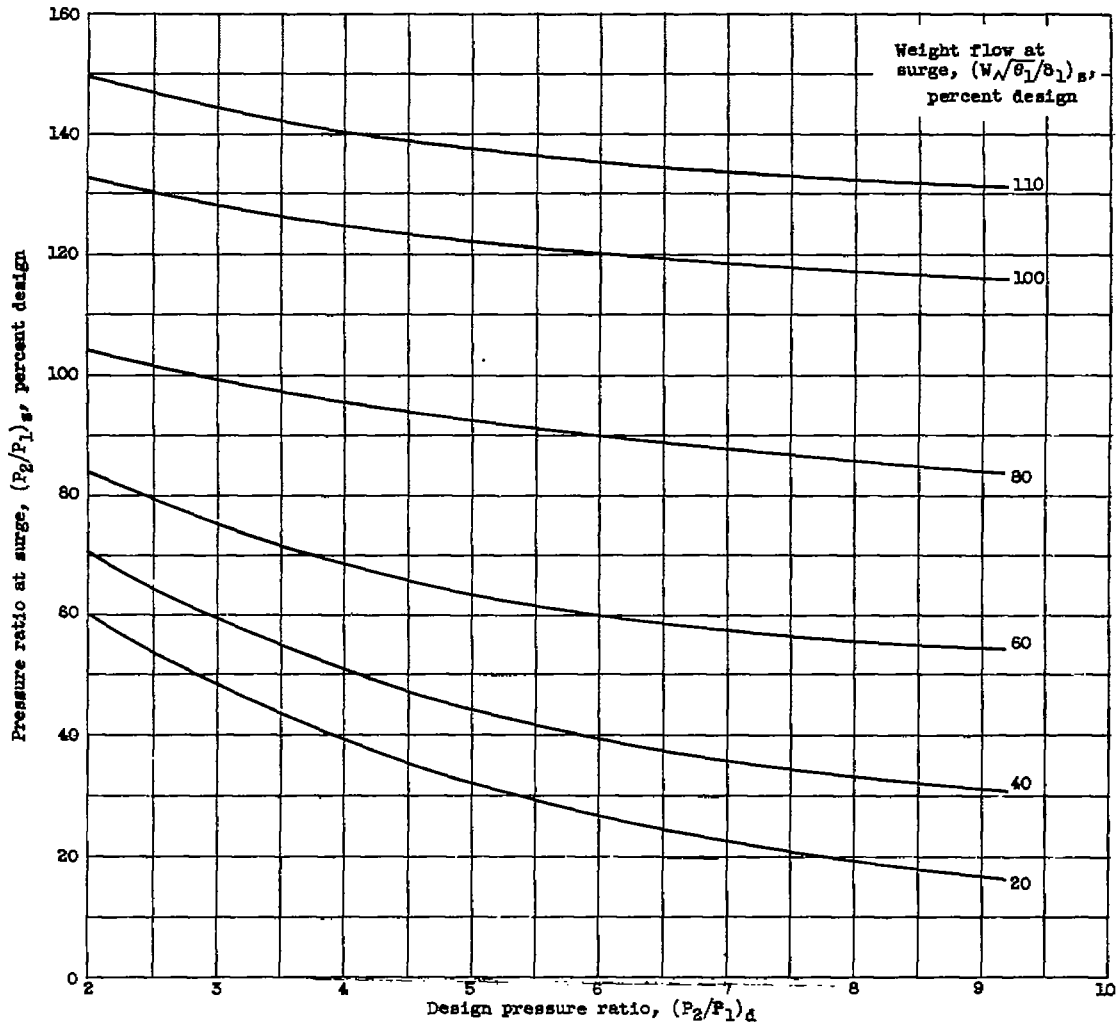


Figure 3. - Effect of design pressure ratio on surge line.

3367

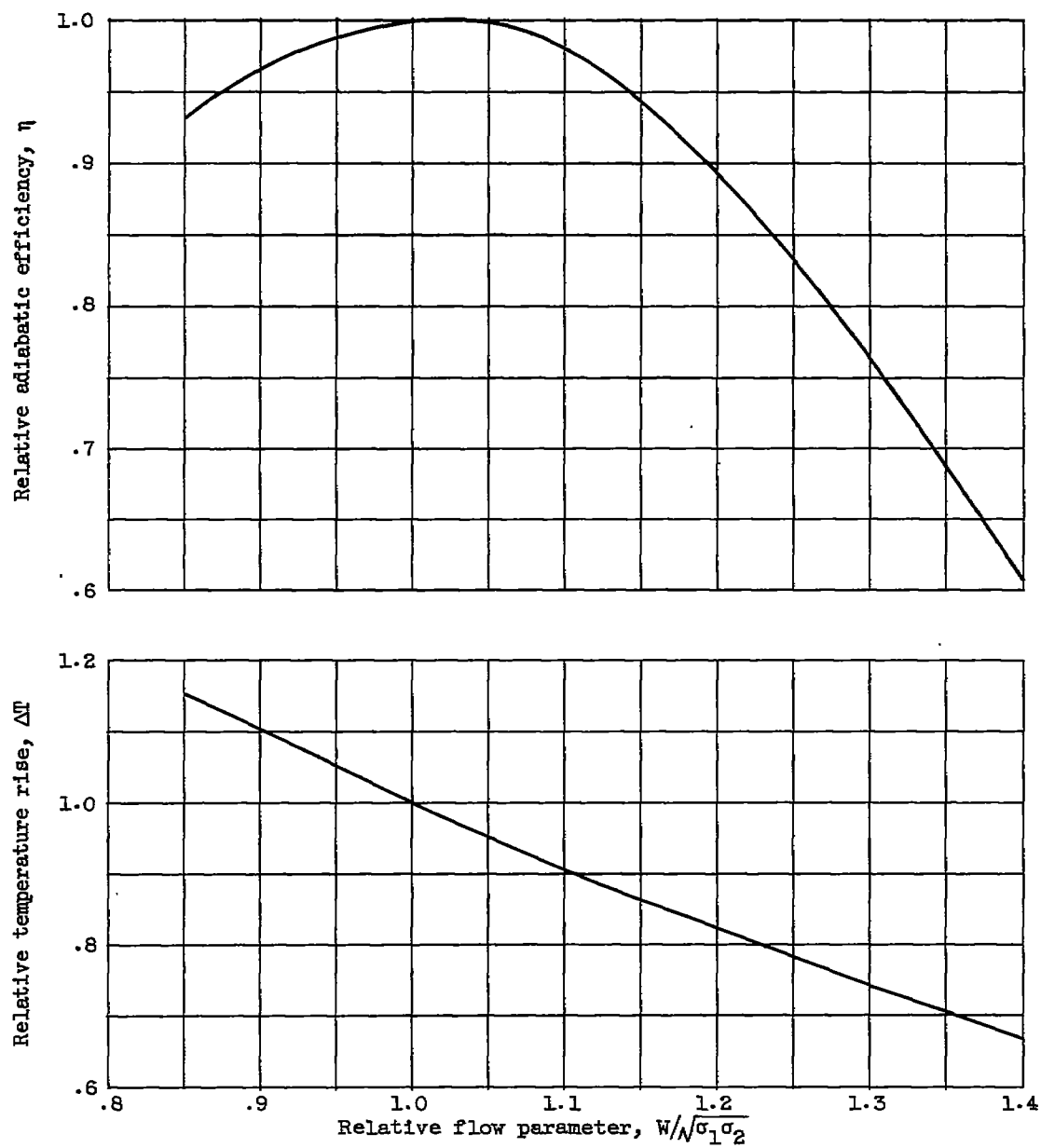


Figure 4. - Constant-speed characteristics relative to backbone conditions.

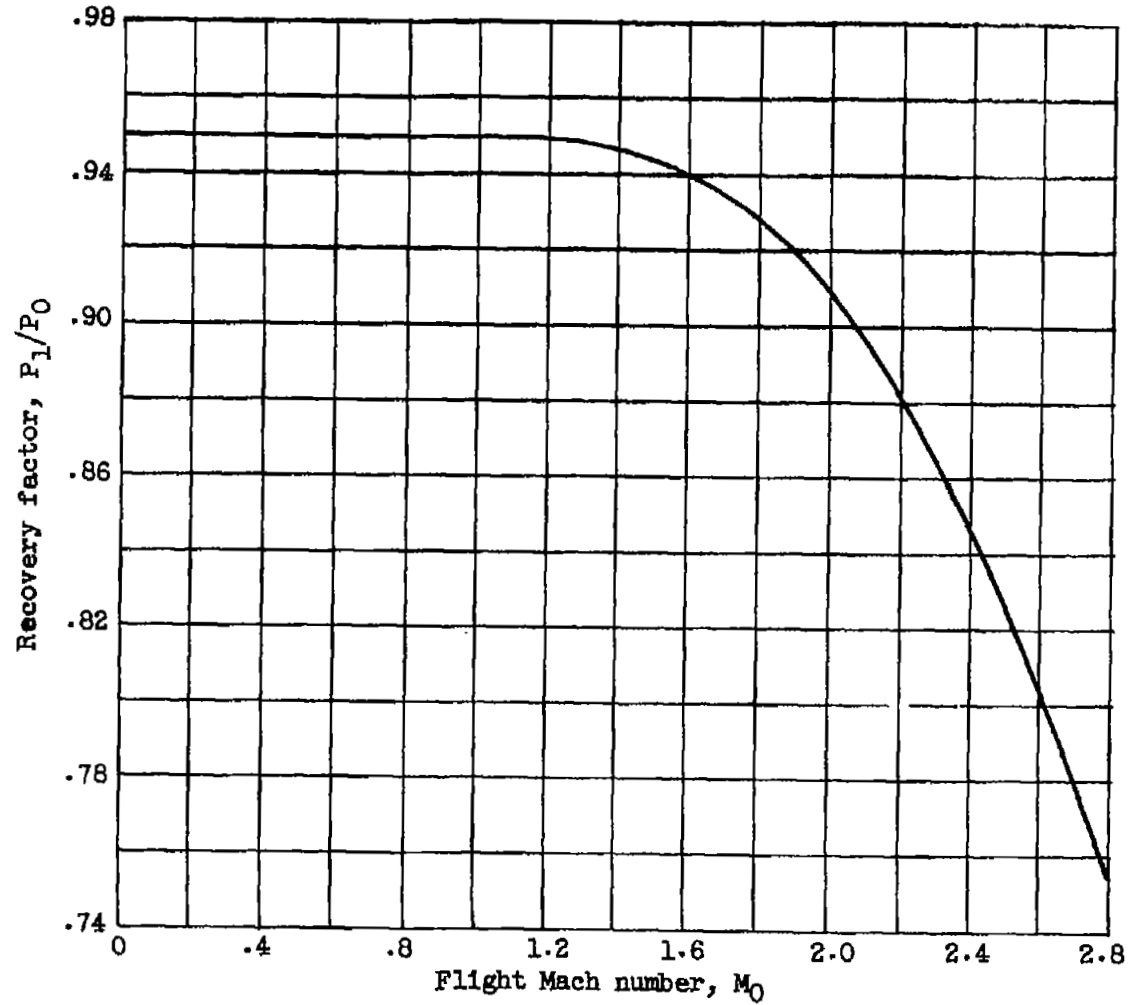
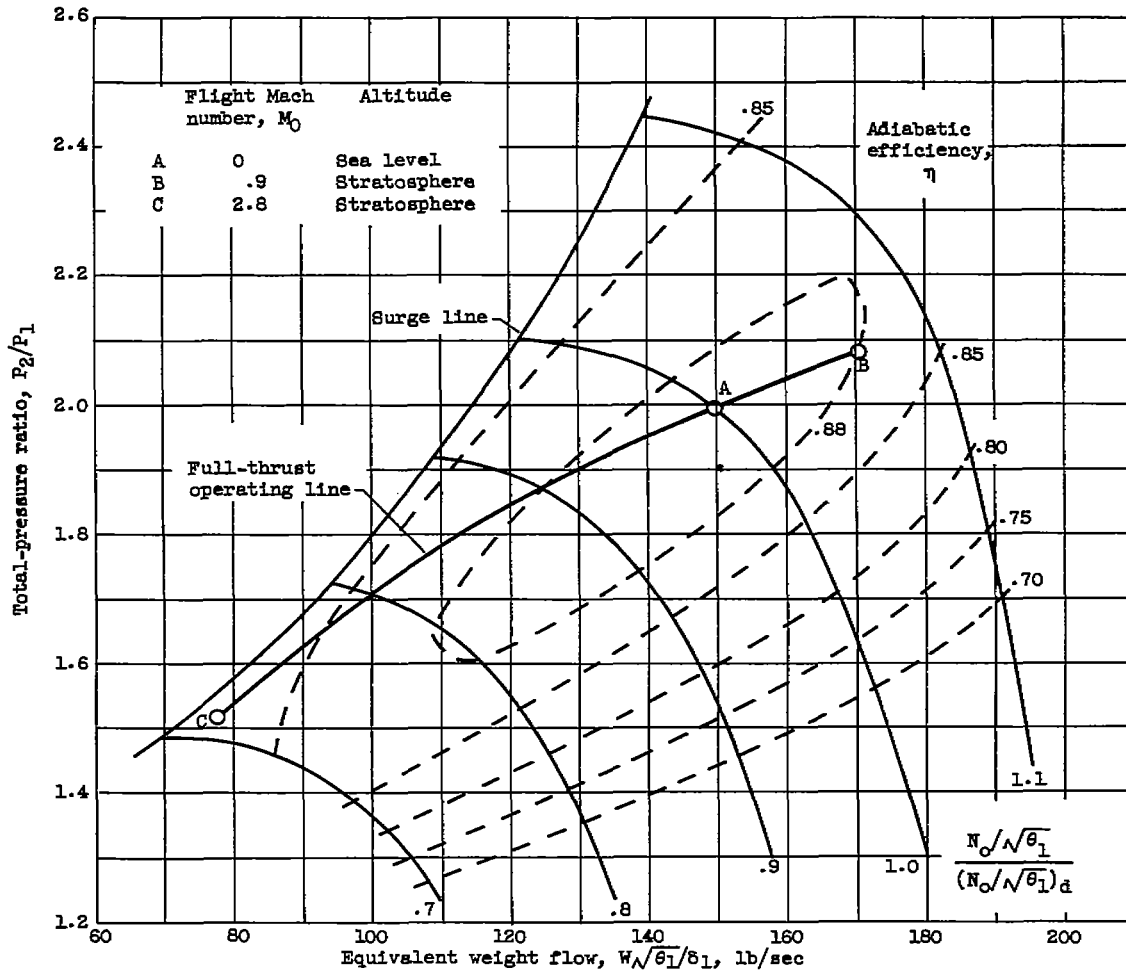


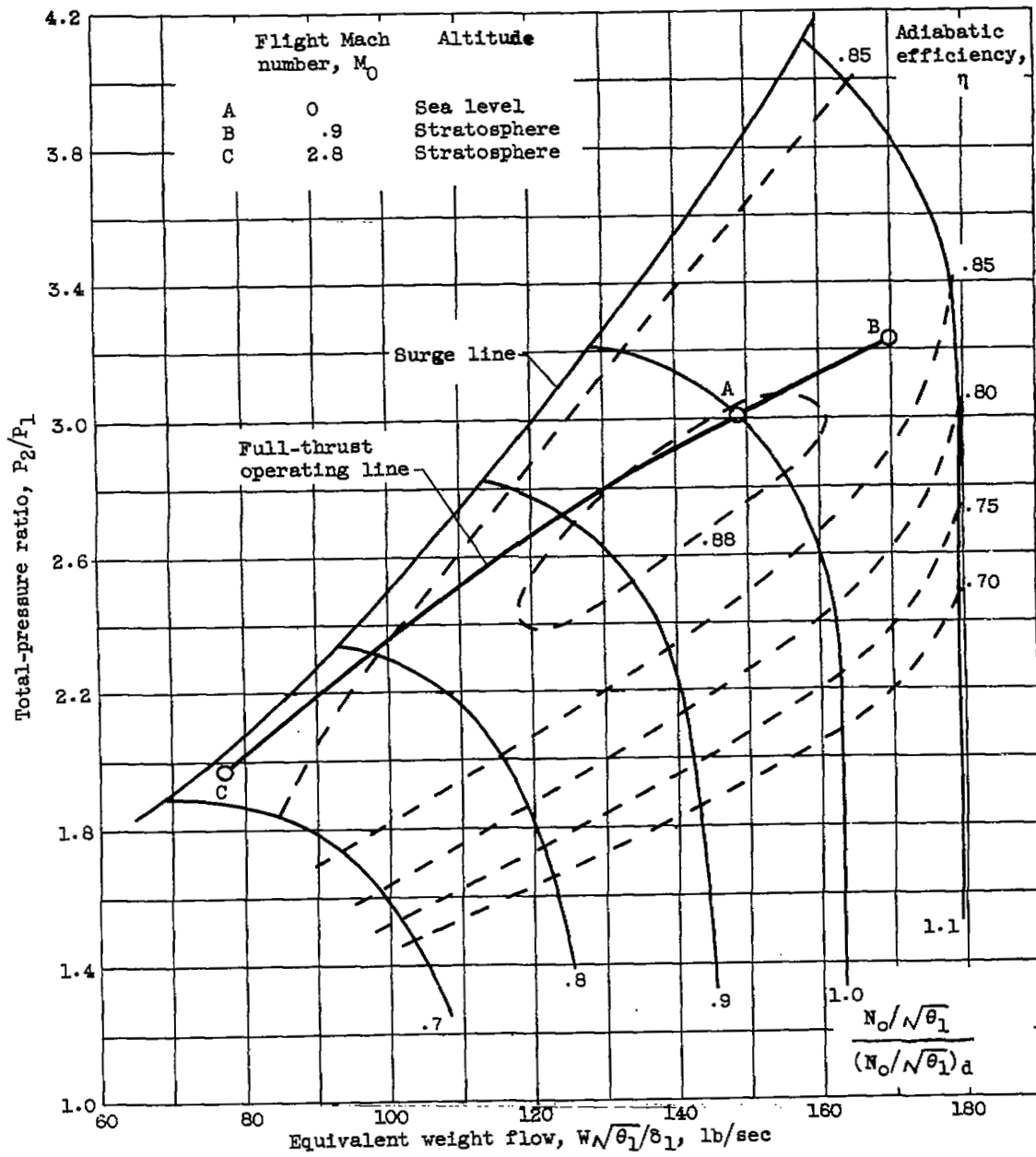
Figure 5. - Performance of inlet used with engines 26, 34, and 43.

3367



(a) Engine 26.

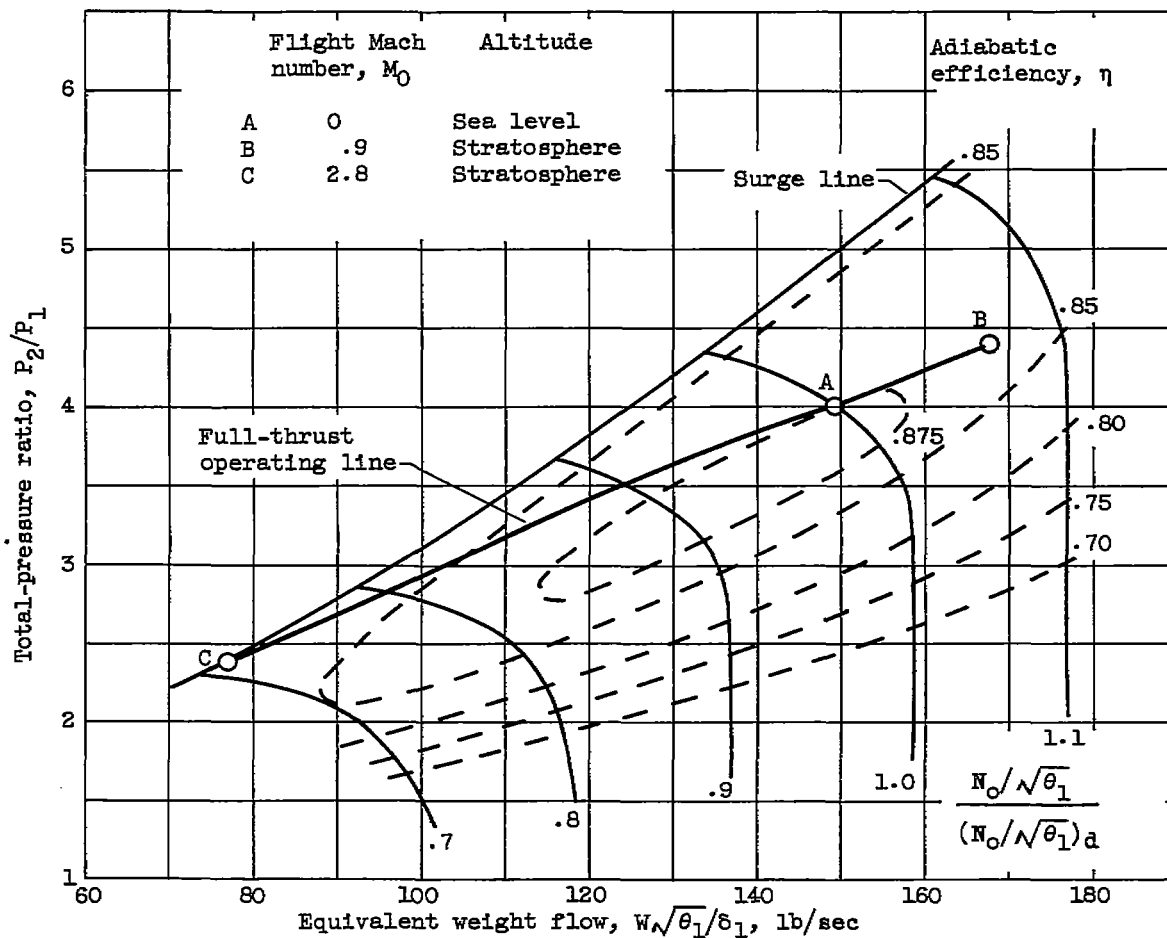
Figure 6. - Outer-compressor performance maps.



(b) Engine 34.

Figure 6. - Continued. Outer-compressor performance maps.

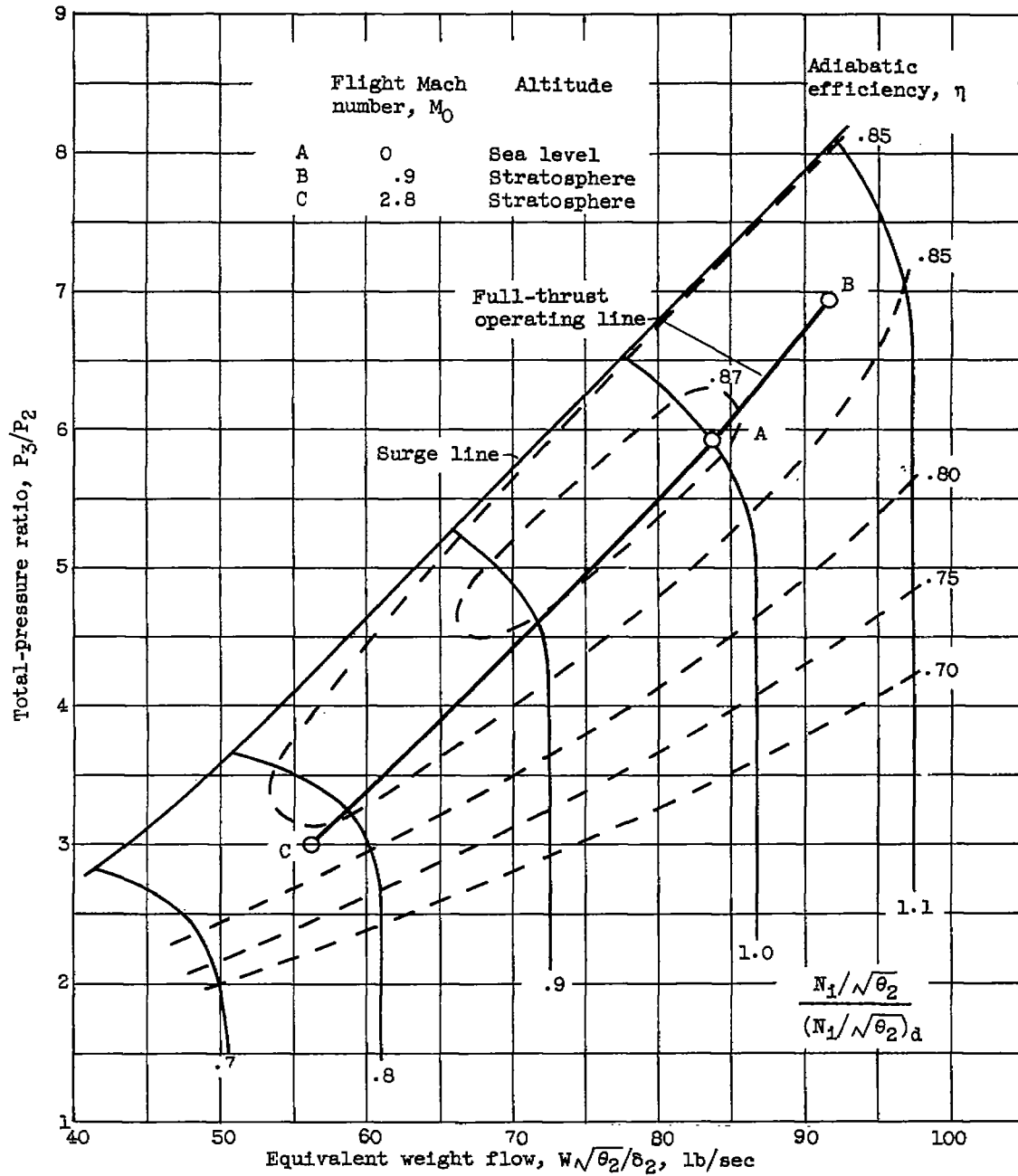
CS-4 3367



(c) Engine 43.

Figure 6. - Concluded. Outer-compressor performance maps.

3367

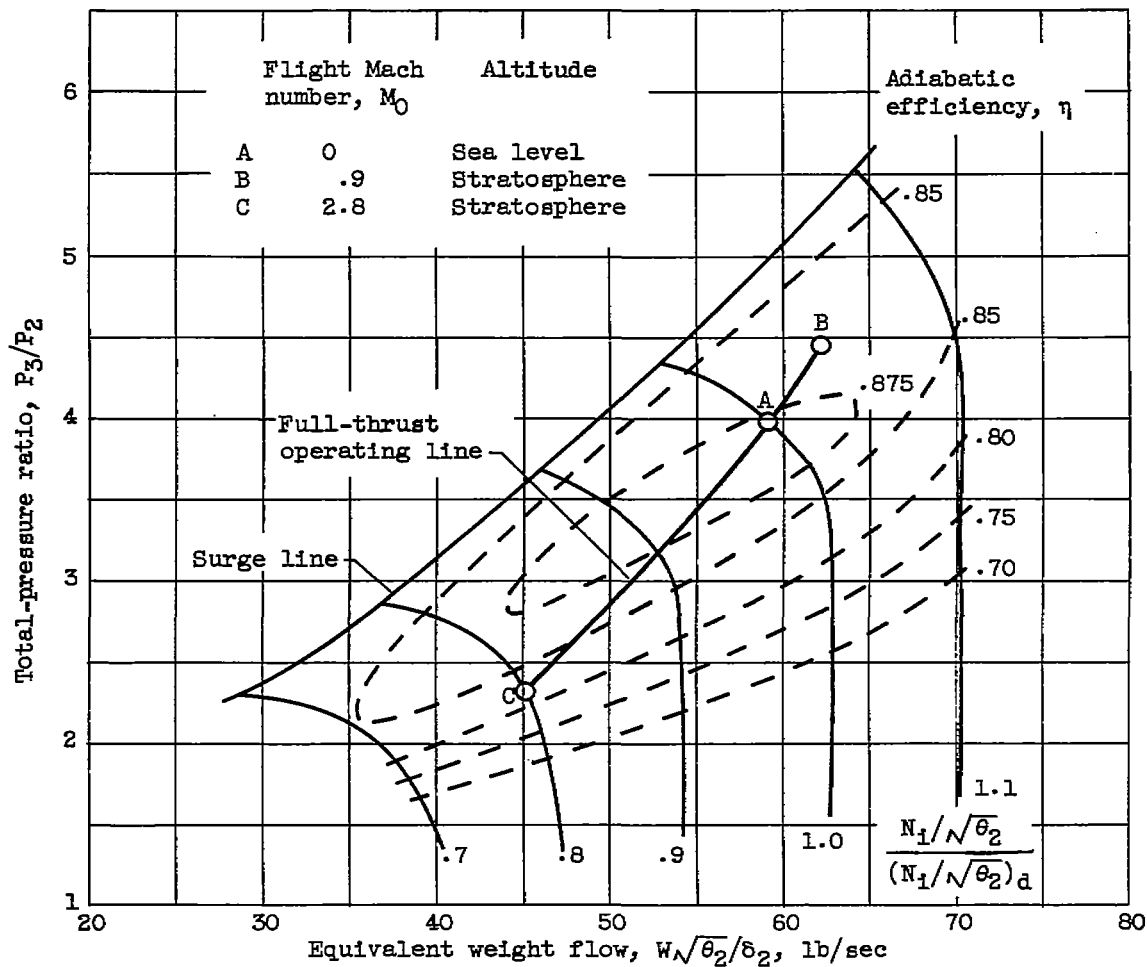


(a) Engine 26.

Figure 7. - Inner-compressor performance maps.

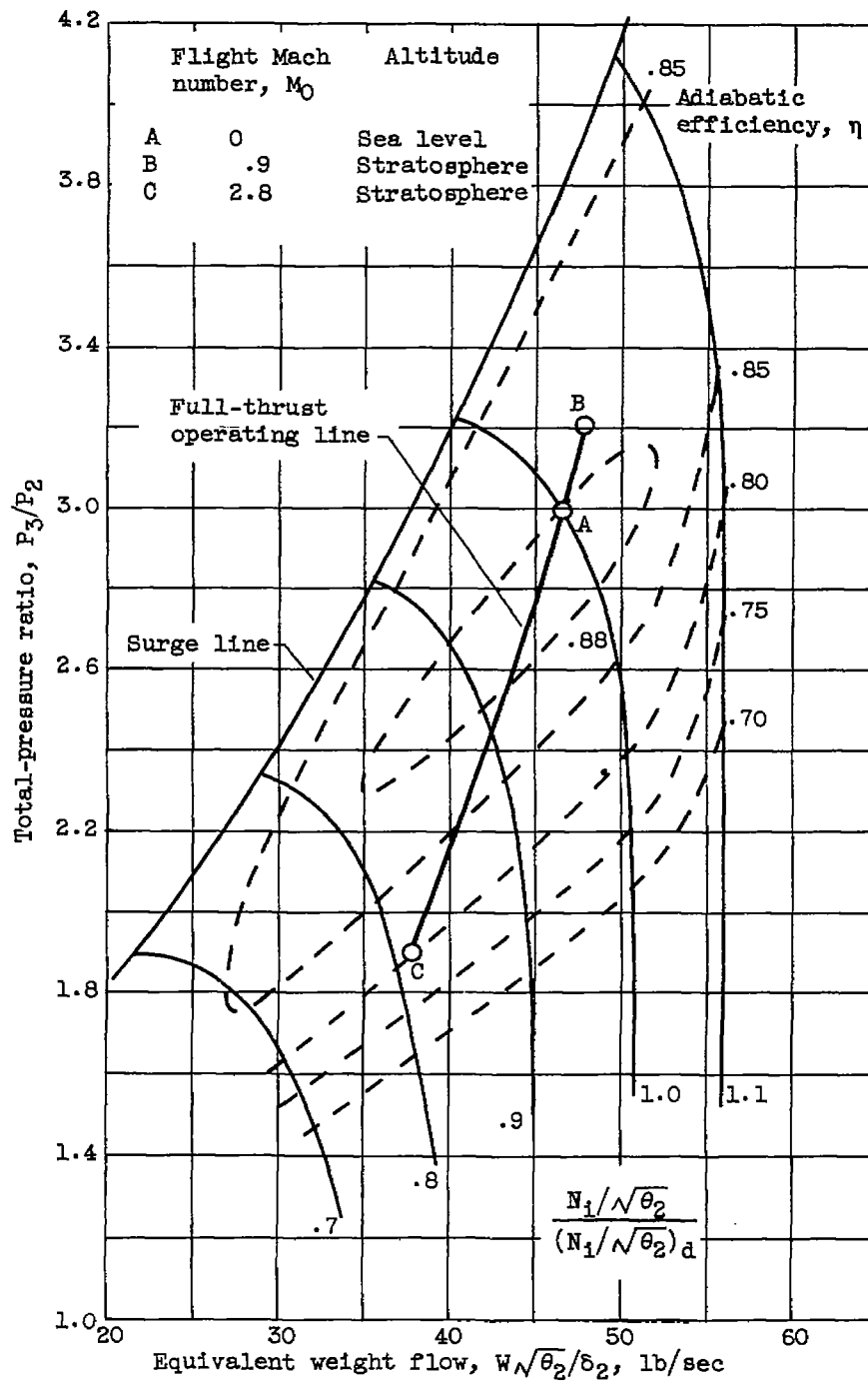
3367

CS-4 back



(b) Engine 34.

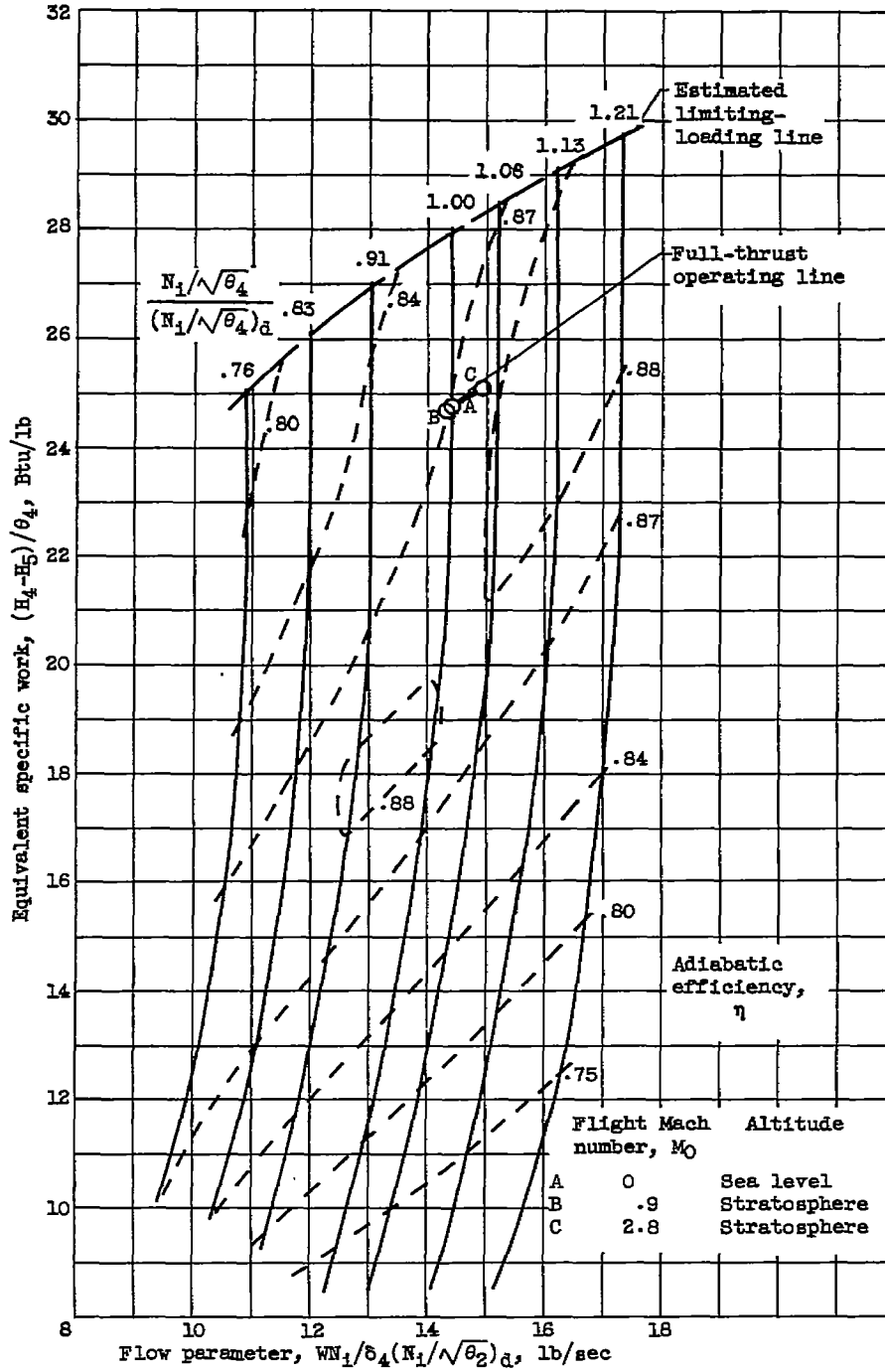
Figure 7. - Continued. Inner-compressor performance maps.



(c) Engine 43.

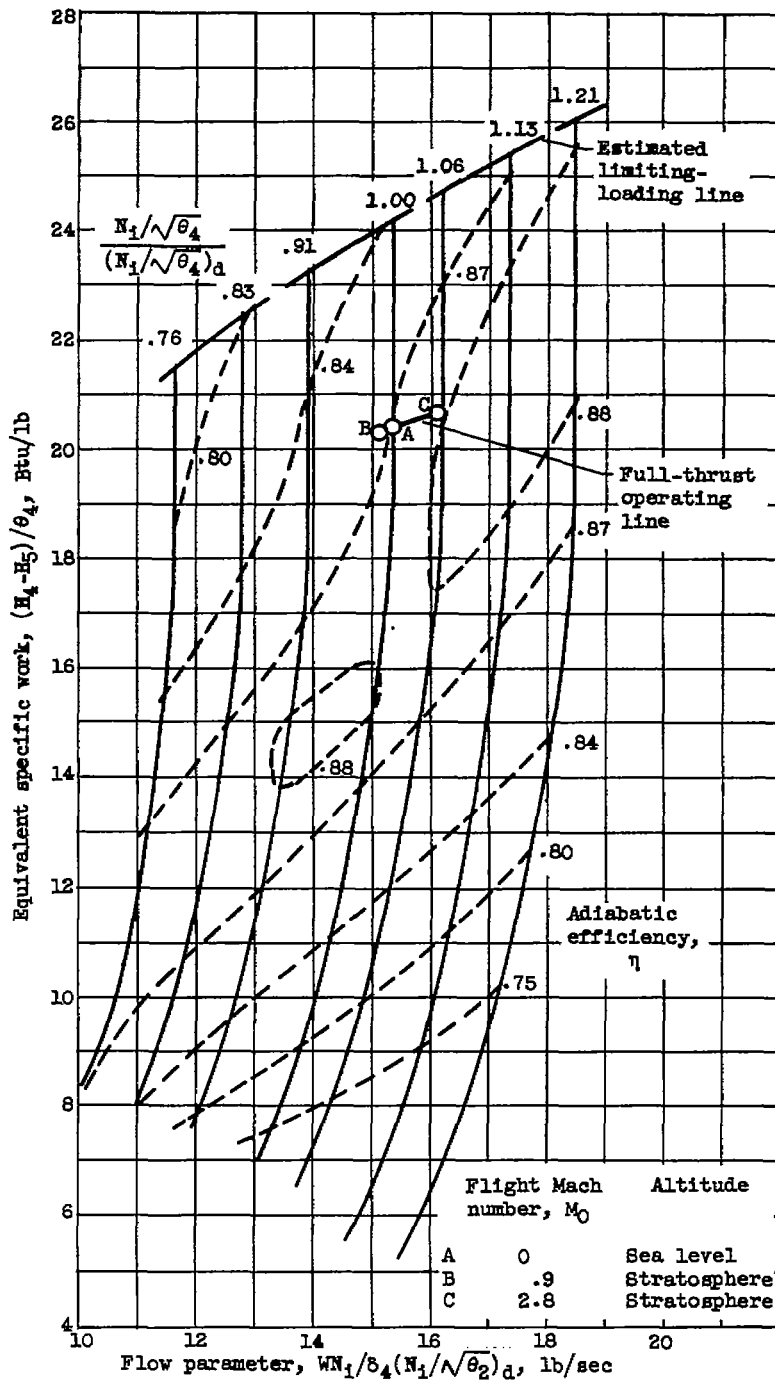
Figure 7. - Concluded. Inner-compressor performance maps.

3367



(a) Engine 26.

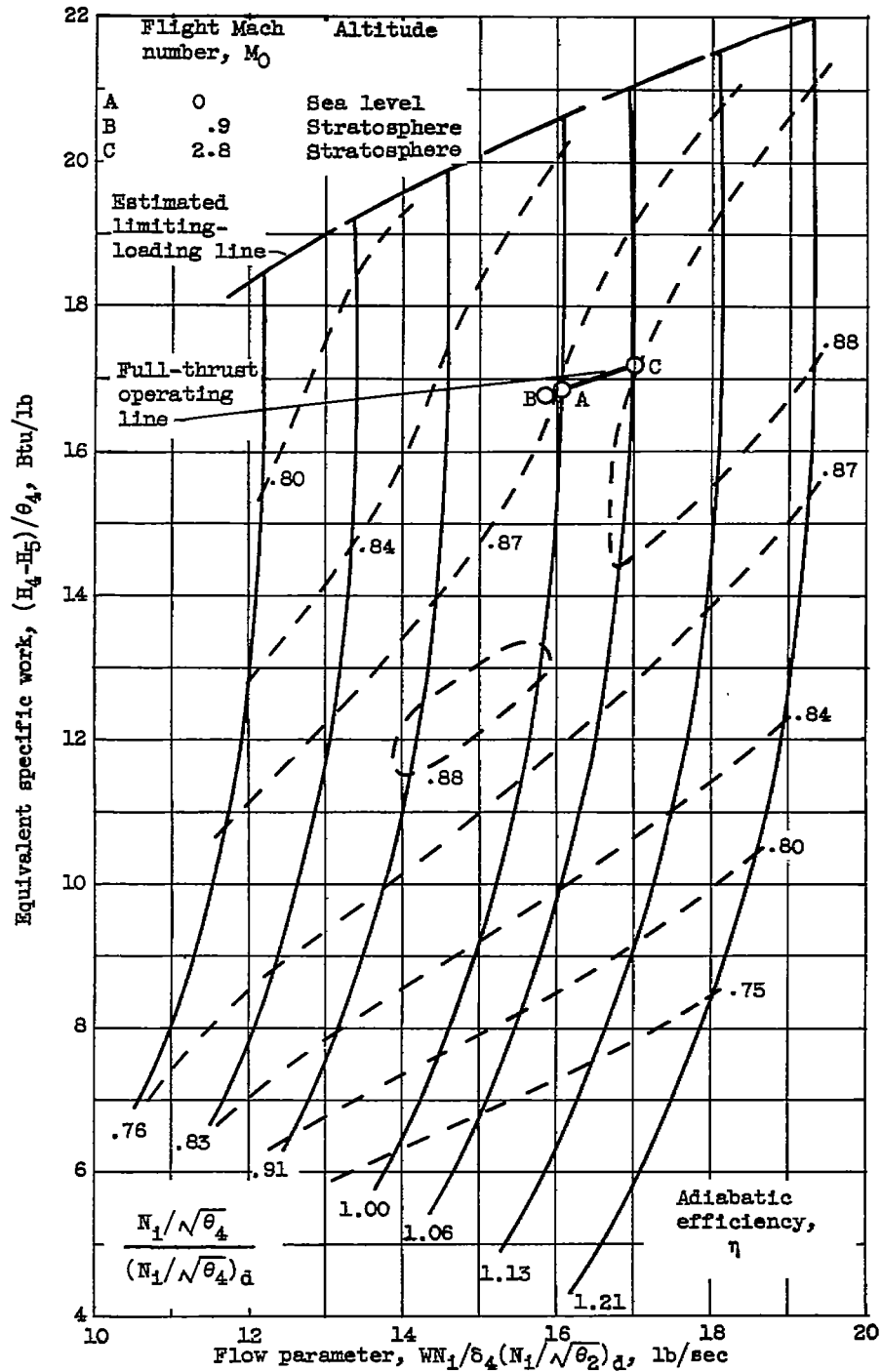
Figure 8. - Inner-turbine performance maps.



(b) Engine 34.

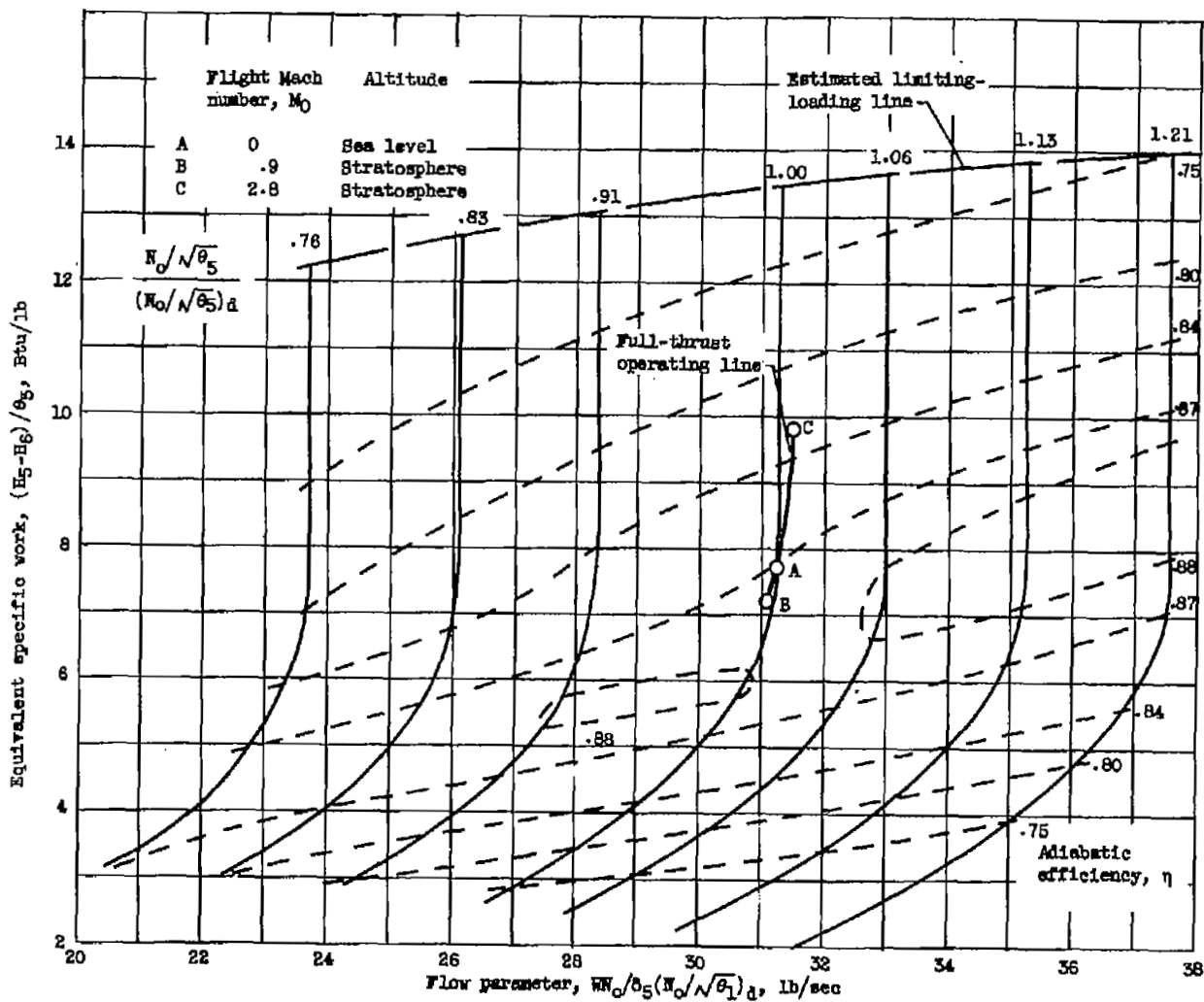
Figure 8. - Continued. Inner-turbine performance maps.

3367



(c) Engine 43.

Figure 8. - Concluded. Inner-turbine performance maps.

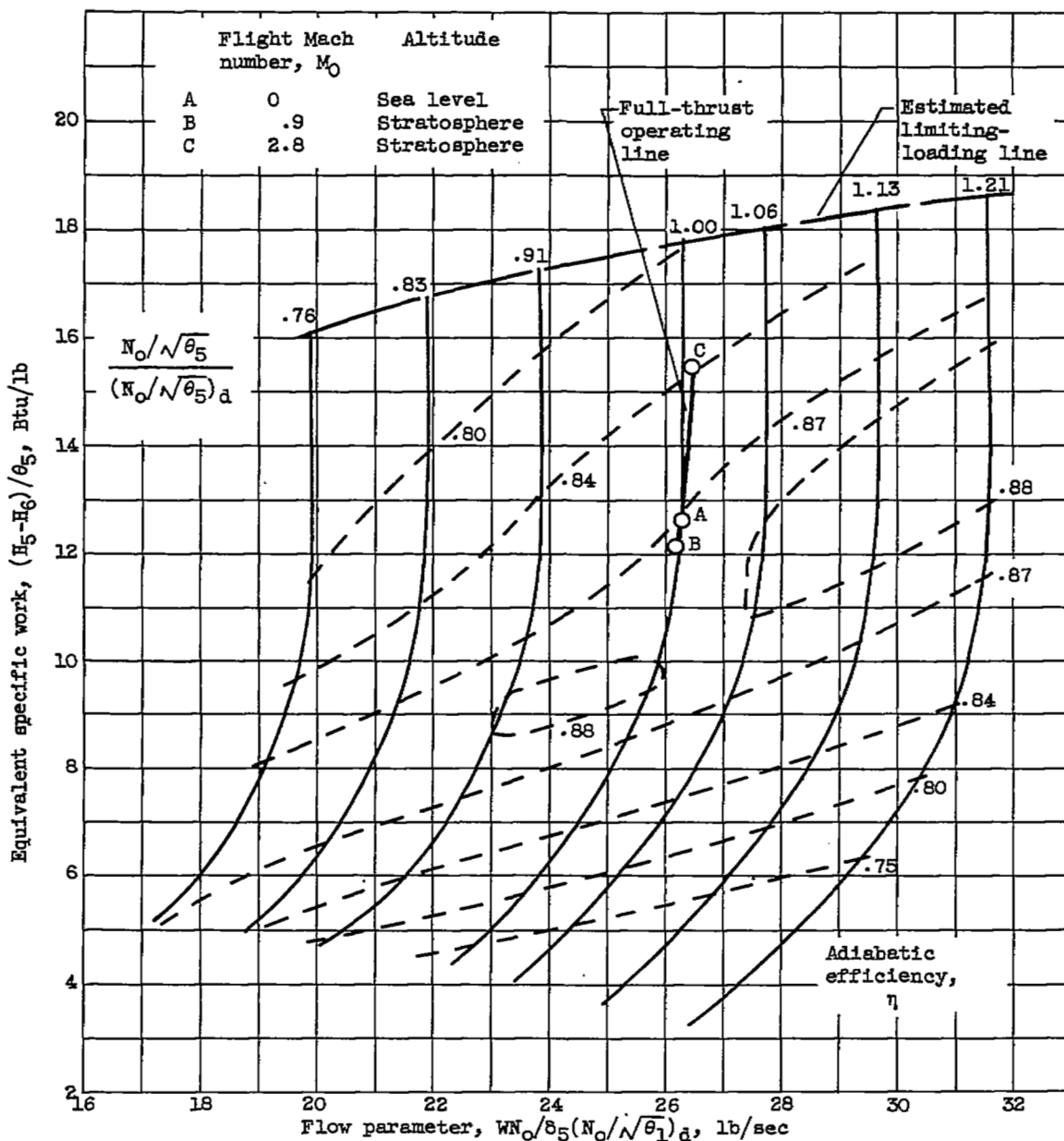


(a) Engine 28.

Figure 9. - Outer-turbine performance maps.

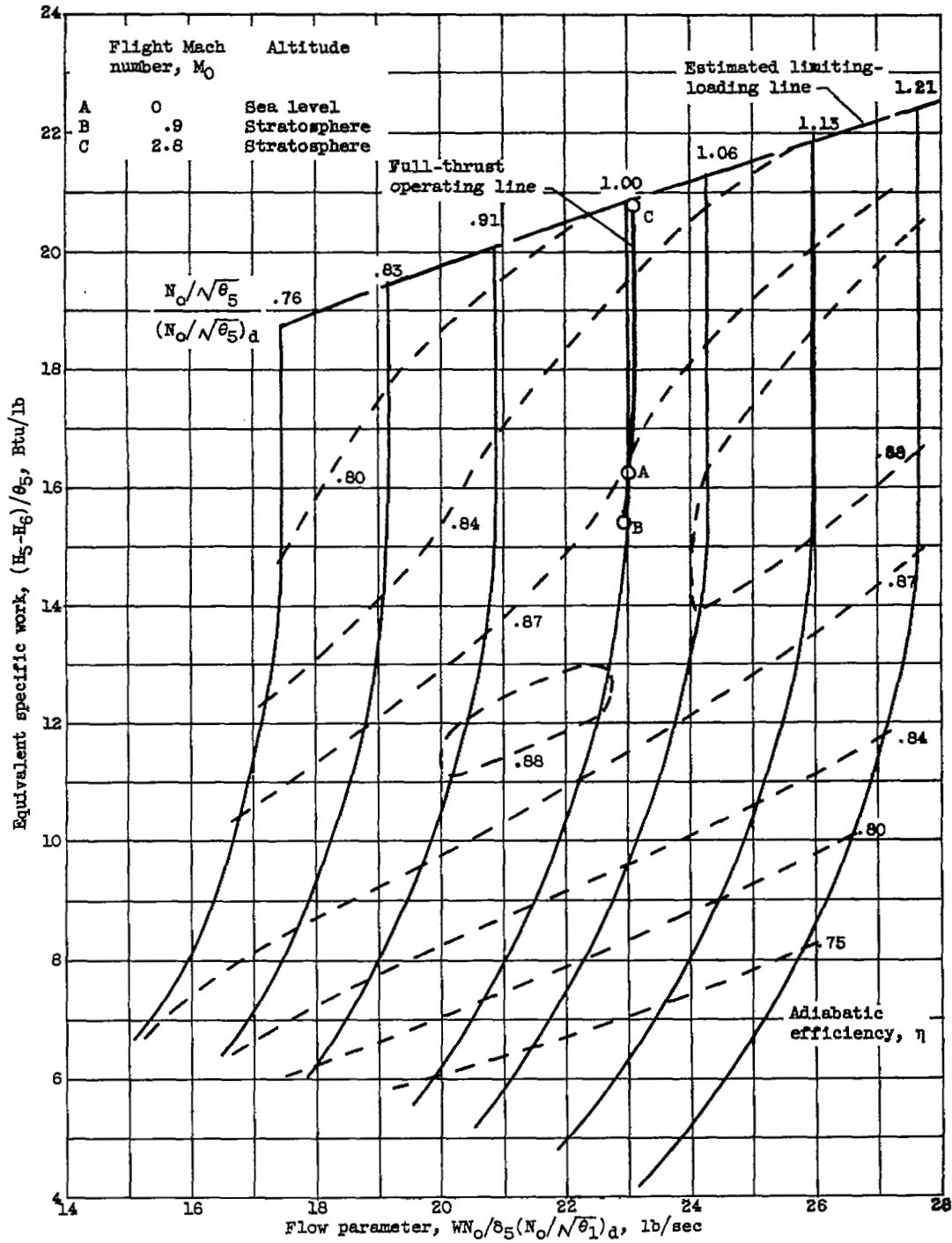
3367

CS-5



(b) Engine 34.

Figure 9. - Continued. Outer-turbine performance maps.

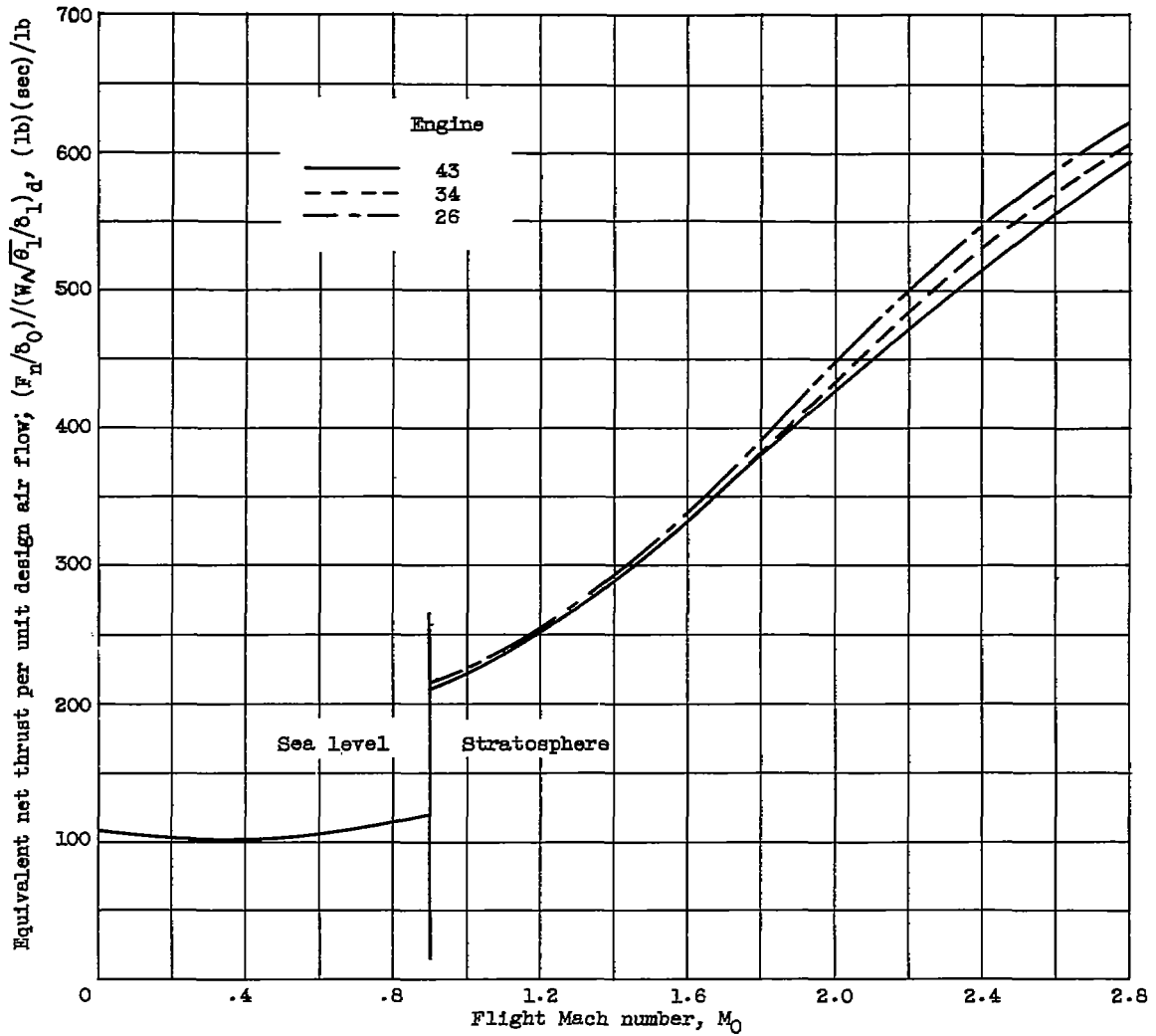


(c) Engine 43.

Figure 9. - Concluded. Outer-turbine performance maps.

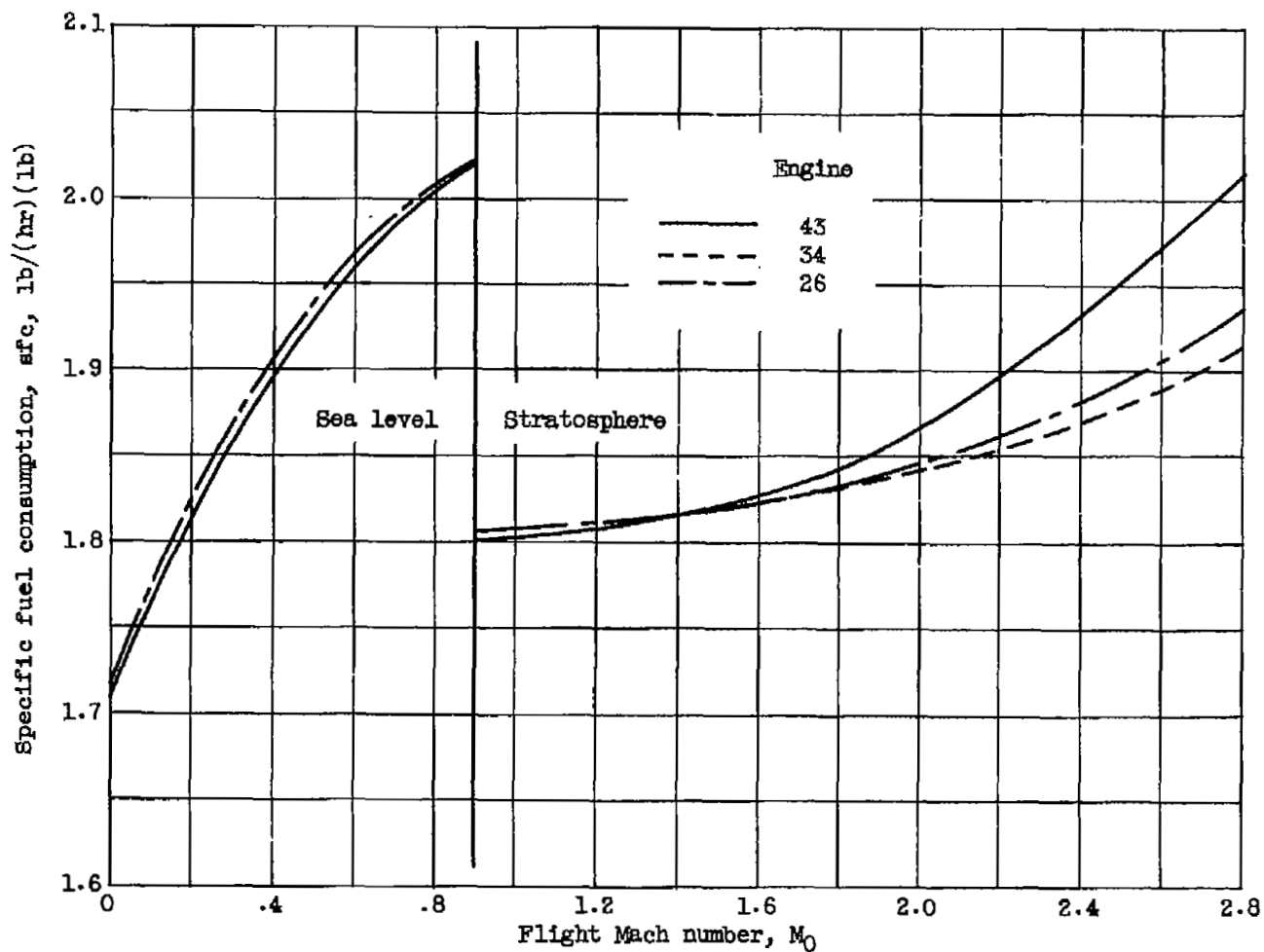
3367

CS-5 back 3367



(a) Equivalent net thrust per unit design air flow.

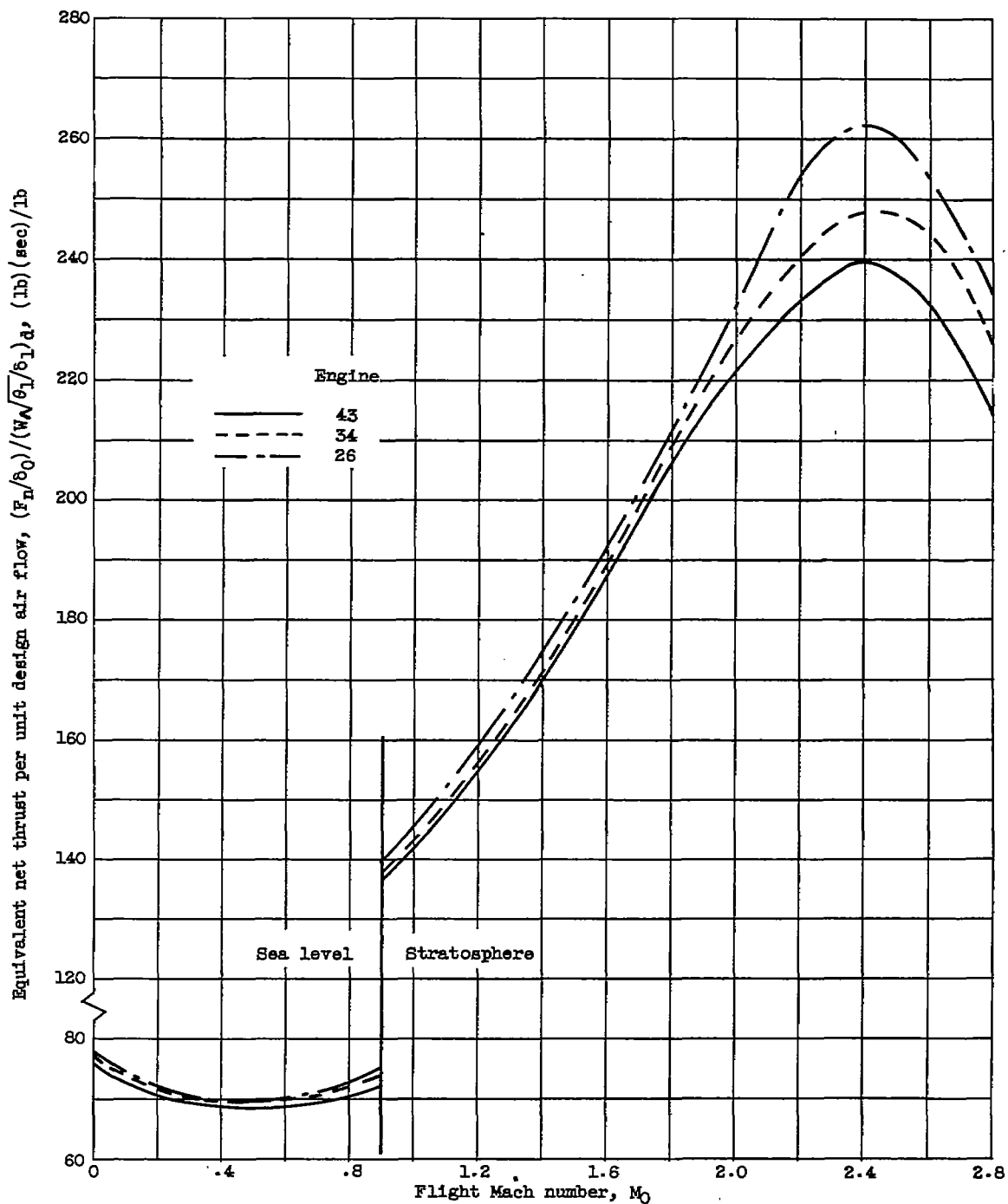
Figure 10. - Full-thrust performance with afterburning for complete exhaust-nozzle expansion.



(b) Specific fuel consumption.

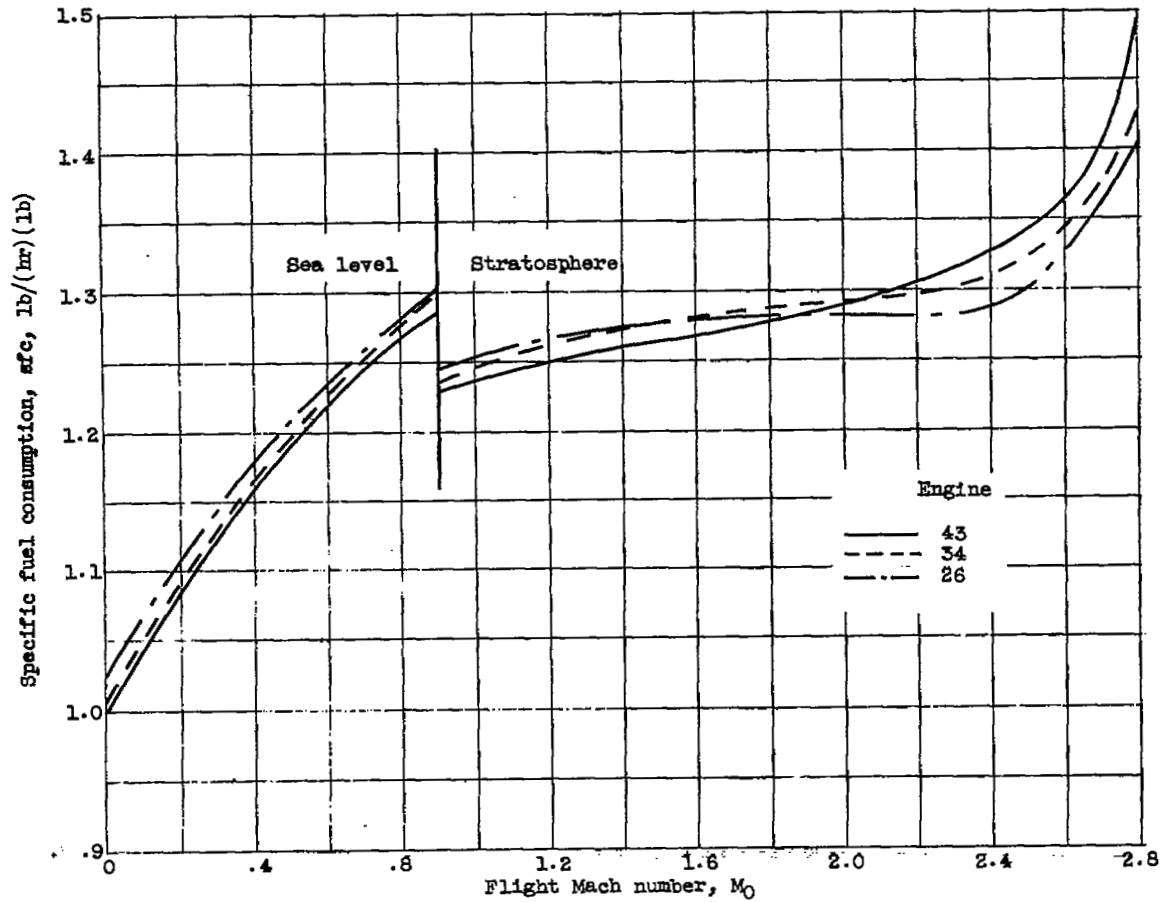
Figure 10. - Concluded. Full-thrust performance with afterburning for complete exhaust-nozzle expansion.

3367



(a) Equivalent net thrust per unit design air flow.

Figure 11. - Full-thrust performance without afterburning for complete exhaust-nozzle expansion.



(b) Specific fuel consumption.

Figure 11. - Concluded. Full-thrust performance without afterburning for complete exhaust-nozzle expansion.

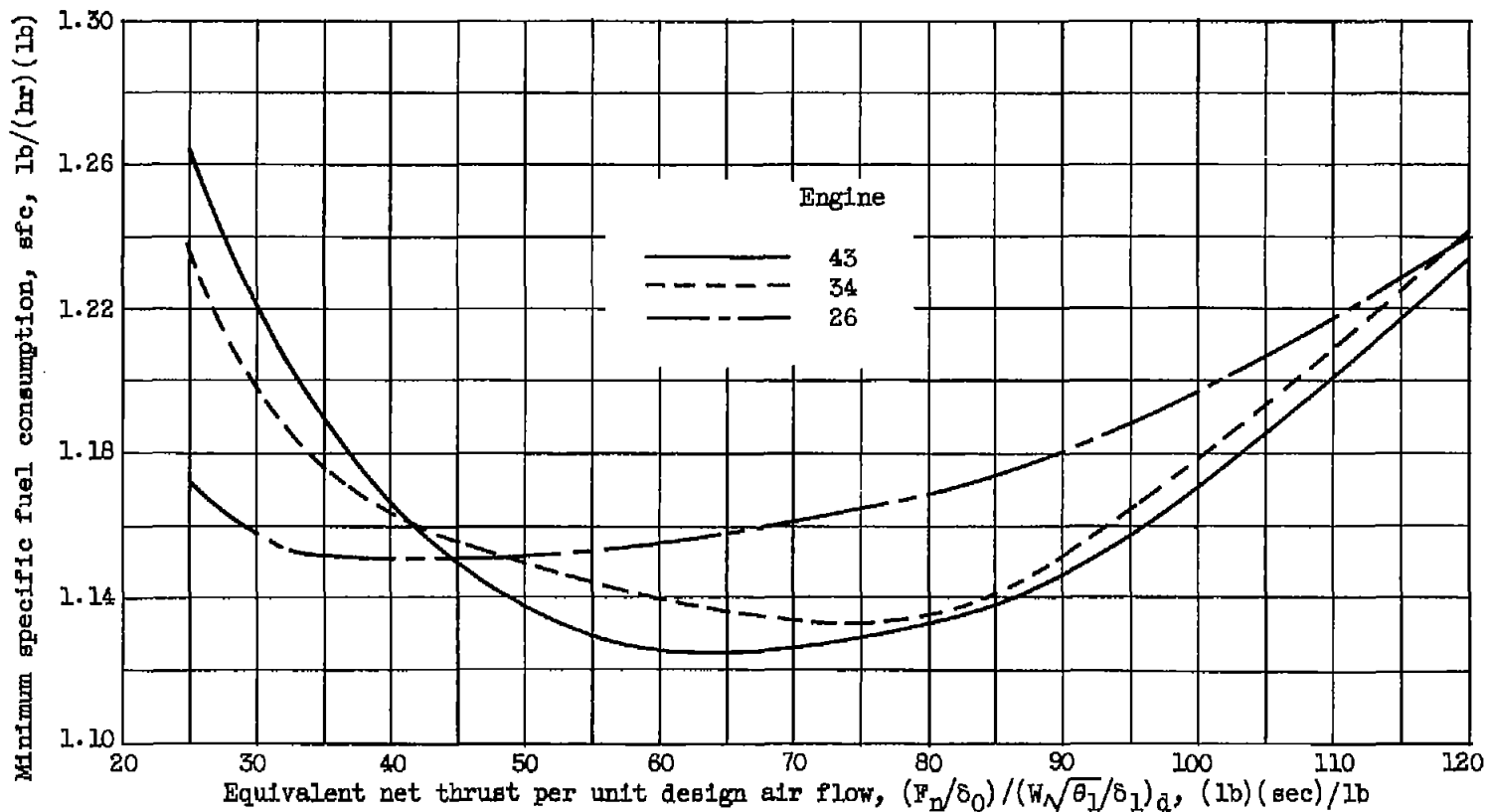
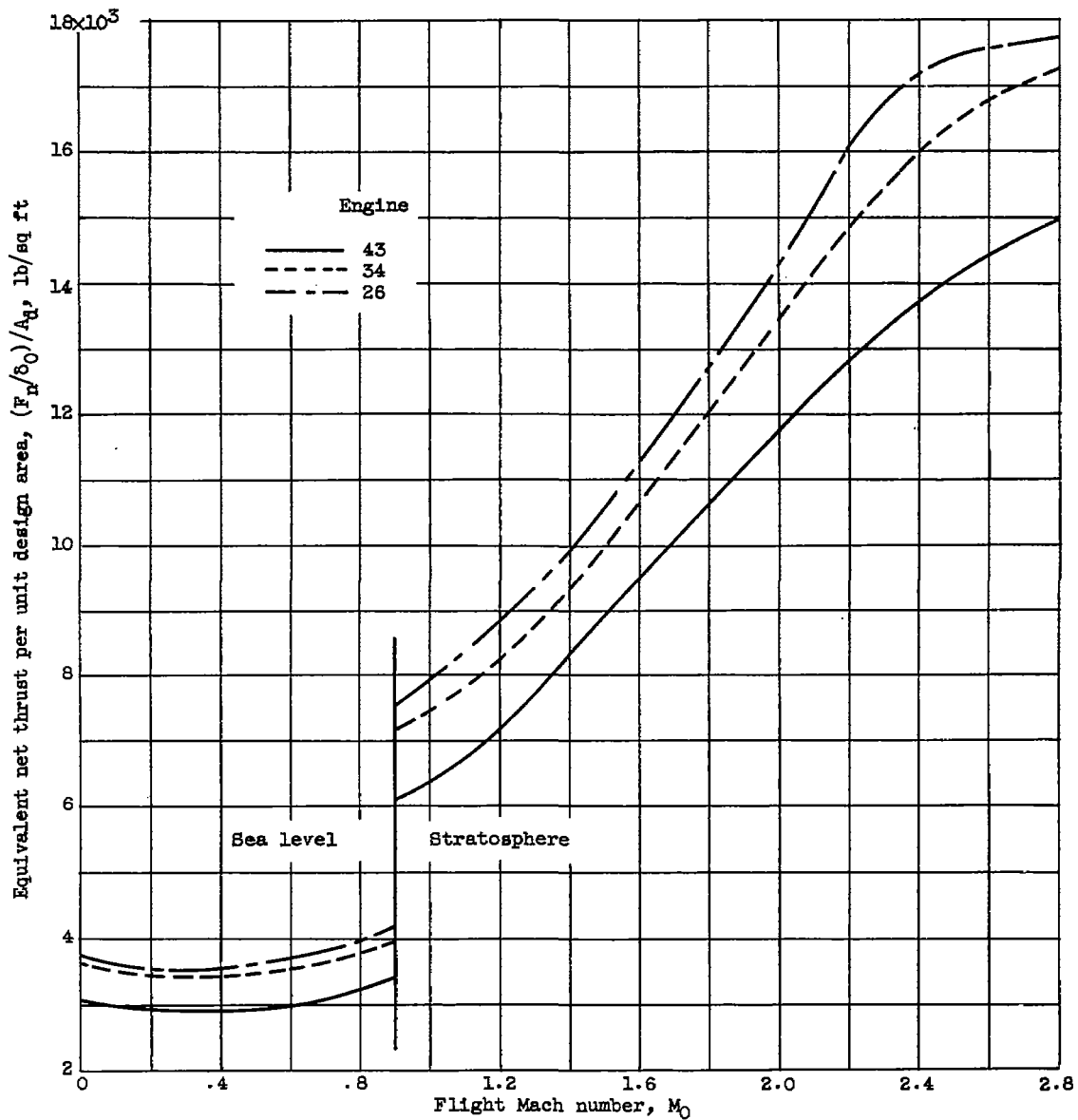
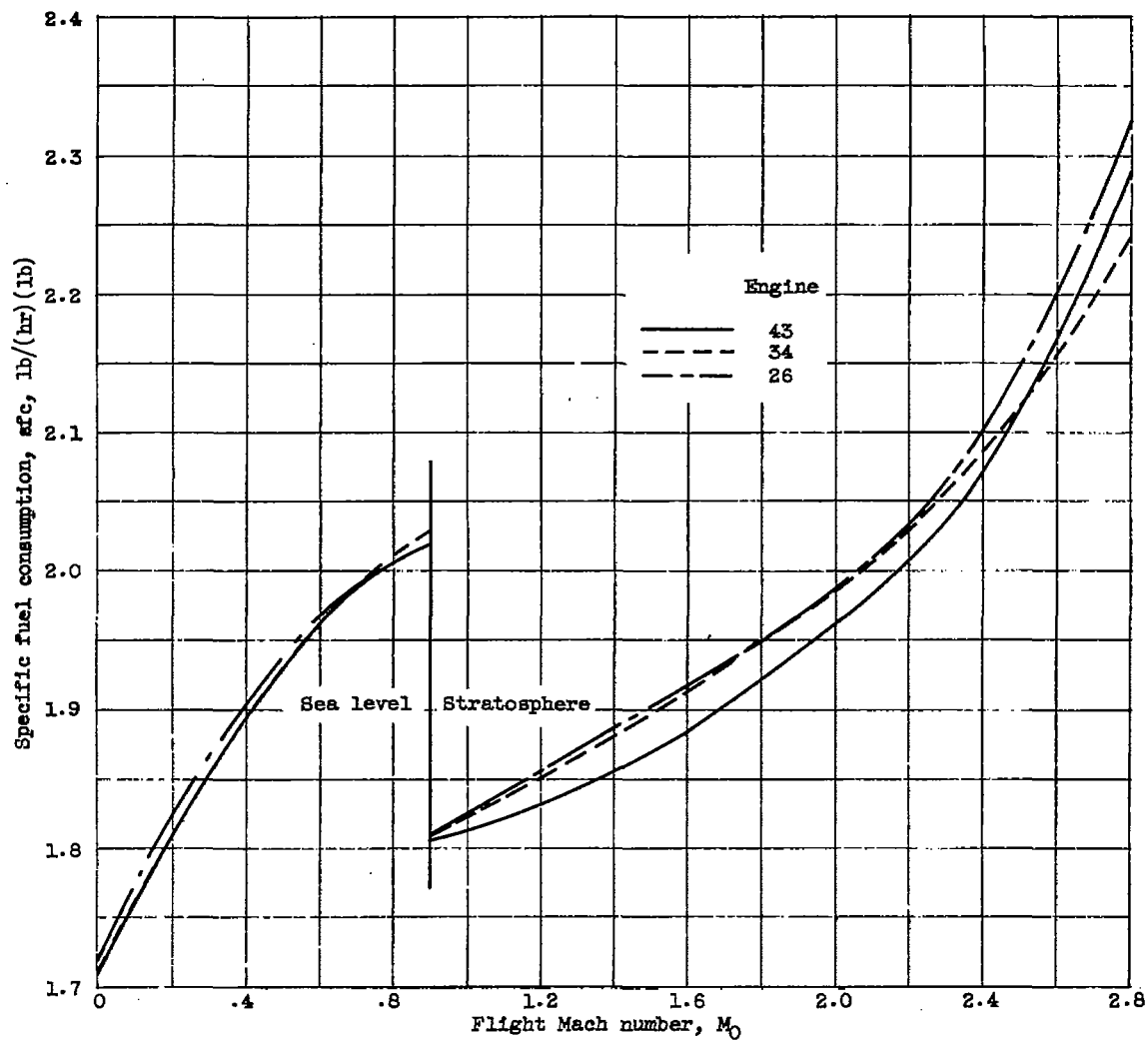


Figure 12. - Cruise performance for complete exhaust-nozzle expansion at Mach 0.9 in stratosphere.



(a) Equivalent net thrust per unit design area.

Figure 13. - Full-thrust performance with afterburning for incomplete exhaust-nozzle expansion.



(b) Specific fuel consumption.

Figure 13. - Concluded. Full-thrust performance with afterburning for incomplete exhaust-nozzle expansion.

NASA Technical Library



3 1176 01435 4238

~~CONFIDENTIAL~~